European Journal of Pharmaceutical Sciences 209 (2025) 107089

Contents lists available at ScienceDirect

European Journal of Pharmaceutical Sciences

journal homepage: www.elsevier.com/locate/ejps

Synthesis and physicochemical characterization of new potential haptens and their precursors with morphine skeleton

Balázs Simon [a,b], István Köteles [a,b], Réka Kovács [a,b], Márta Kraszni [a,b], Péter Horváth [a,b], Sándor Hosztafi [a,b], Károly Mazák [a,b,*]

[a] Semmelweis University, Department of Pharmaceutical Chemistry, Hőgyes E. u. 9., H-1092 Budapest, Hungary
[b] Center for Pharmacology and Drug Research & Development, Department of Pharmaceutical Chemistry, Semmelweis University, Budapest, Hungary

ARTICLE INFO

Keywords:
Opioids
Haptens
Physicochemical properties
Acid-base properties
Lipophilicity
B-cyclodextrin complex

ABSTRACT

Opiate analgetics are widely used therapeutic agents, but their side-effects can cause serious harm to users, and they are often abused for their euphoric effects. Their abuse is a serious healthcare problem worldwide, and in addition, pharmacological treatments of this disorder possess serious problems such as adverse effects, medication adherence complications, and relapse to addiction after the therapy. One possible way to combat the latter issue would be vaccination with macromolecule-opiate conjugates. Therefore, novel compounds are necessary not just as potential therapeutic agents, but also as new hapten-like molecules. In this work, we present the synthesis of novel N-cyanoalkyl- and N-aminoalkyl-noropiate derivatives, which could be used either as new therapeutic agents or haptens.

An important aim of this work was to quantify biorelevant physicochemical properties (basicity, lipophilicity) of the newly synthesized compounds. The determination of the protonation macroconstants characterizing the acid-base properties was performed by pH-potentiometry. To determine the partition coefficients, we used the shake-flask method with different octanol/water phase ratios. The complex formation of the pharmacologically active N-cyanoalkyl derivatives with β-cyclodextrin was also investigated. The stoichiometry of the β-cyclodextrin complexes was determined by the Job's plot method, their structure by NMR spectroscopy, and their stability by NMR and circular dichroism spectroscopy. The study of this complex opens up the possibility of a more in-depth formulation investigation. The species-specific basicity of the new potential aminoalkyl haptens was also characterized, which can help further structure-activity relationship studies.

1. Introduction

1.1. Importance of morphine derivatives

As of today, morphine (**1**) and its derivatives are widely used therapeutic agents, when it comes to pain management of end-of life patients, mainly suffering from cancer, or patients suffering from chronic pain. For this reason, they are on the Essential Medications List published by the World Health Organization. (WHO EML 23rd List, 2023). Their high effectiveness unfortunately comes with several serious side-effects. The most concerning property is their high abuse potential, which leads to misuse of numerous opiates, most notably heroin (3, 6-diacetylmorphine hydrochloride) (**2**), and oxycodone (**3**) (Fig. 1). Misuse of these compounds is an ever-growing problem, especially in the US. (Humphreys et al., 2022; Judd et al., 2023; Volkow and McLellan, 2016)

Dealing with this on-going crisis is limited. Although multiple therapeutic options exist - the use of methadone, buprenorphine, naltrexone - and their effectiveness is well documented, they require good compliance from the patient, usually supported by non-pharmaceutical therapy as well. (Lee et al., 2015; Mumba et al., 2018) It has to be highlighted, that these therapeutic options do not protect the patient from relapse, that usually leads to overdose and death.

1.2. Immunization against drugs of abuse

A possible additional therapeutic option would be immunization against the abused drugs, which could serve as a supplementary therapy.

* Corresponding author.
E-mail addresses: simon.balazs@semmelweis.hu (B. Simon), kraszni.marta@semmelweis.hu (M. Kraszni), horvath.peter@semmelweis.hu (P. Horváth), hosztafi.sandor@semmelweis.hu (S. Hosztafi), mazak.karoly@semmelweis.hu (K. Mazák).

https://doi.org/10.1016/j.ejps.2025.107089
Received 30 January 2025; Received in revised form 27 March 2025; Accepted 30 March 2025
Available online 31 March 2025

Small-molecule drugs of abuse are generally not immunogenic themselves, therefore an immunogenic carrier molecule is needed, to which the small molecules can be chemically attached. This drug-macromolecule conjugate can then be used in vaccines, and after immunization, drug-specific antibodies are formed by the immunized body. (Bremer and Janda, 2017) These drug derivatives are called haptens, and this strategy was rather successfully used in the case of cocaine and nicotine. (de Villiers et al., 2010; Ramakrishnan et al., 2014) In the case of opiates, a morphine-6-hemisuccinate (**4**) hapten (Fig. 2) was designed as early as 1974, and it was shown to alter self-administration of heroin in a Rhesus monkey. (K. F. Bonese et al., 1974)

1.3. Opioid haptens

Since then, a number of various opioid haptens were synthetized, using different sites for modification on the morphine skeleton. This includes introducing functional groups which can react with the immunogenic proteins, mainly carboxyl, amino, and thiol groups by functionalizing the hydroxyl groups or changing the substituent of the N-17 nitrogen (Anton et al., 2009; Gutman et al., 2021; Herndon et al., 1976; Hosztafi et al., 2024; Jalah et al., 2015; Pravetoni et al., 2012; Richard T. Brown et al., 1995; Sulima et al., 2018), and in one case, the C-2 aromatic site was modified through diazotization. (Gross et al., 1974) The position of attachment of the haptens to the carrier is important, as this will determine the face of the conjugated molecule that will be shown to the immune system. This will have a major influence on the selectivity of the vaccination (Findlay et al., 1981), and the ability to recognize different drugs and their effective metabolites. This is especially important in the case of heroin, it can undergo rapid hydrolysis by the esterases in the body, forming 6-acetylmorphine. (Findlay et al., 1981; Herndon et al., 1976; Matyas et al., 2014) So far it seems that the best recognition towards the changes in the 3, and the 6 positions can be achieved with haptens that are attached to the carrier through the nitrogen of the piperidine ring. (J. Beike et al., 1998) Designing haptens directly against known active metabolites is also possible, the most important one is the 6-glucuronide, although these were usually used for specific immunoassays. (Brown et al., 1995)

Another fact to consider is that haptens themselves can get metabolized, which can alter the ability of the vaccine to block the effect of the targeted molecule. To combat this, more metabolically stable analogues were designed, containing amino groups in place of the hydroxyl groups at C-3 and C-6 respectively. These amino groups can be used to react the molecule with the linker at either of those sites, or to show them to the immune system, by linking the analogue at the N-17 place. (Sulima et al., 2018) Hydrolysis of the haptens can also happen at the linker, especially when an ester group is used. Therefore, the use of an amide group is critical, because it is much more stable. (Bremer et al., 2017; Stowe et al., 2011) The C-14 site is especially important, when the targeted drug of abuse is not heroin, but oxycodone, which differs from heroin in the (i) C-3 methyl ether, (ii) the C-6 ketone, (iii) the saturated C-7–8 bond and (iv) a hydroxyl group added to the C-14 site. A hapten, which is bonded to the C-6-group effectively shows these sites of the drug, and this proved to be effective, while not altering other important opioids' ability to exert their effects. (Pravetoni et al., 2012) Using this site to produce anti-heroin haptens proved to be less successful but can

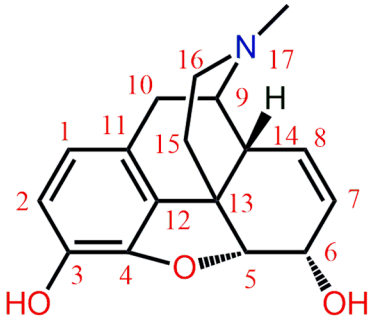

(1)

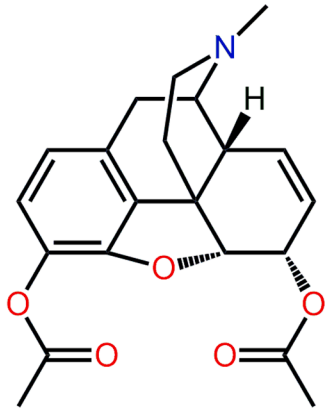

(2)

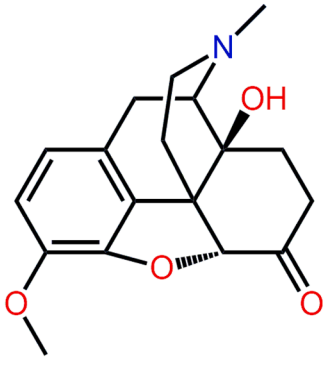

(3)

Fig. 1. Structure of morphine (**1**), heroin (**2**), and oxycodone (**3**).

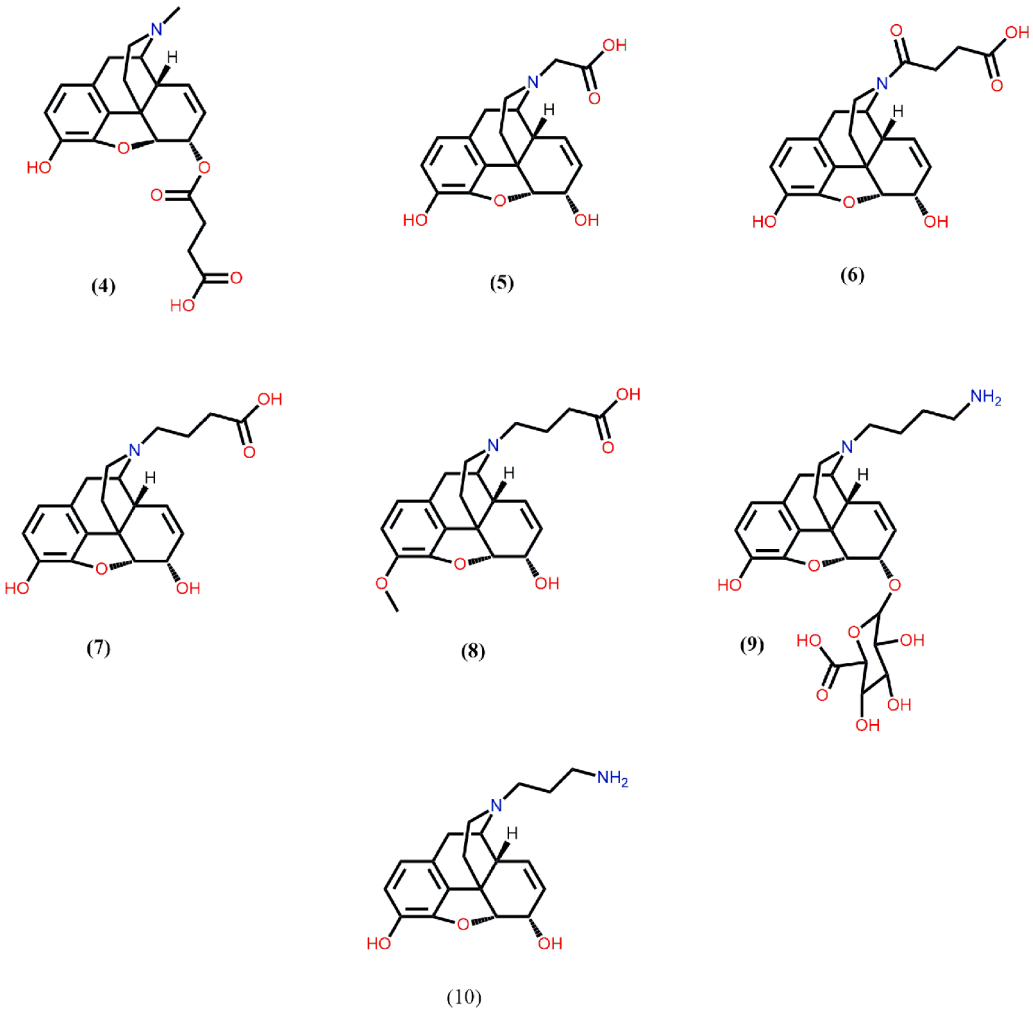

Fig. 2. Structures of a few important opiate haptens.

serve as a useful starting point for future work. (Gutman et al., 2021) A more useful formulation used an aminobutyl side chain at the piperidine nitrogen in oxycodone. This hapten was able to protect mice from overdose. (Kimishima et al., 2017)

With the data of these studies in hand, it was concluded that the most effective way to elicit structure-selective immune response against heroin and its metabolites is binding the hapten molecule to the carrier through the substituent of the nitrogen of the piperidine ring. The other important factor is the use of an amide bond in the linker. (Bremer et al., 2017; Stowe et al., 2012)

1.3.1. Haptens linked at the N-17-substituent

Designing haptens with a morphine structure linked through the substituent of the N-17 site was started as early as 1976, when N-carboxymethyl-normorphine (**5**) was synthetized. This was then coupled to bovine serum albumin (BSA) with the mixed anhydride method, but this failed to produce antiserum in any animals tested. (Herndon et al., 1976)

N-succinyl-normorphine (**6**) was prepared in 1985 (Aherne and Littleton, 1985), for measuring morphine with an immunoassay, and it was found to be effective at producing morphine-specific antisera, outperforming morphine-6-hemisuccinate. In 1981, N-carboxypropyl-normorphine (**7**) and N-carboxypropyl-norcodeine (**8**) were prepared. Antisera raised by these haptens conjugated to BSA were able to discriminate between structural changes at the C-3-; and C-6-positions, as well between changes made at the C-14 position. (Findlay et al., 1981) In 1993, the N-butylamino-normorphine hapten was synthetized, which showed minimal cross reactivity with codeine. (Usagawa et al., 1993) In 1995, a nitrogen-coupled hapten series was developed where a free primary amino group was introduced. The synthesis proceeded from normorphine, reacting it with 4-trifluoroacetamidobutanal in the presence of sodium cyanoborohydride in ethanol. This was coupled with the appropriate glucuronide imidate and yielded the morphine hapten (**9**), which was then used to produce the codeine derivative. Reduction of the double bond in the morphine skeleton also yielded the appropriate dihydro derivatives. (Brown et al., 1995)

In 1998, N-propylamino-normorphine (**10**) was synthetized for usage in a radioimmunoassay, through alkylation of normorphine with trifluoro-acetamidopropylbromide, and then deprotecting this derivative with sodium hydroxide in methanol to acquire the hapten, which was then coupled to activated BSA. (J. Beike et al., 1998)

1.4. Opiate agonists with non-methyl substituent on nitrogen

Usually, the introduction of a substituent other than the naturally occurring methyl group at the nitrogen of the piperidine ring in opiates causes the activity of the compound to diminish or even turn into an antagonistic effect. Mixed agonist/antagonist-type molecules, like nalbuphine, where the substituent is a cyclobutylmethyl group, and full antagonist molecules, like naloxone and naltrexone are used in treating an overdose, or for treating opioid use disorder. Introducing bigger, more rigid substituents in this position usually leads to either antagonist effect, or a loss of receptor binding, exemplified by the N-phenethyl substituent, which leads to effective opioid receptor agonists. (Haddou et al., 2014; Wang et al., 2020) The introduction of a cyanoalkyl group

onto the nitrogen can lead to compounds with agonist activity at the opioid receptors (May et al., 2000), with bonding affinity similar to the parent compounds. (Wang et al., 2020) Their other use comes from the fact that the cyano-group is a useful synthon for a primary amine, and therefore these compounds can also be used in preparation of hapten-like derivatives, and other medicinally useful opioid derivatives, for example non-central nervous system acting opioids. (Subasinghe et al., 2004)

Some compounds with a beta-amino group in the substituent of the nitrogen in the D ring are also agonists or partial agonists at the opioid receptors, while some others are antagonists. This is mostly guided by the substituent of the C-14 atom, in this case, the 14-OH substitution led to antagonist compounds. (Ötvös et al., 2023)

1.5. Physicochemical characterization

An important aim of this work was to quantify biorelevant physicochemical properties (basicity, lipophilicity) of the newly synthesized compounds. Acid-base properties determine the charge of a molecule at a given pH that affects all other relevant physicochemical properties, namely lipophilicity, solubility and permeability in medicinal chemistry. This work examines proton transfer processes from the perspective of proton association and utilizes log *K*, the logarithm of the protonation macroconstant. (Mazák and Noszál, 2016)

Lipophilicity is typically quantified by the log *P* value, the logarithm of the partition coefficient. The distribution coefficient (*D*) is a measure of the ratio of concentrations when more than one electrical species are present in solution. It considers the intrinsic lipophilicity of the various electrical species (p_i), and their mole fractions in the aqueous phase (x_i)

$$D = \sum x_i p_i \quad (1)$$

Cyclodextrins (CyDs), a group of oligosaccharides formed by glucose units bound together in a ring, can form complexes with drug molecules and improve their physicochemical properties and thus are frequently referred to as enabling pharmaceutical excipients (Loftsson and Duchêne, 2007; Saokham et al., 2018)

The Job-plot method, named after its first describer, has long been used to determine the stoichiometry of cyclodextrin complexes. Although it was first used to describe metal-ligand molecular complexes, its application has since spread widely to other fields of science, such as in biochemistry for the characterization of protein complexes or the cyclodextrin complexes we studied. (Ingham, 1975; Huang, 1982; Huang et al., 2002)

The structure and stability constants of the complexes were investigated by NMR and circular dichroism measurements to open up the possibilities for additional formulation studies.

2. Materials and methods

2.1. Materials and general procedures

The reagents were purchased from Sigma-Aldrich (St. Louis, MO, USA) Alfa Aesar (Haverhill, MA, USA) and TCI Europe (Zwijndrecht, Belgium) and used without further purification. Solvents were freshly distilled prior to use and were dried over anhydrous Na_2SO_4. ^1H and ^{13}C NMR spectra were recorded on a Varian Mercury Plus (400.0 MHz for ^1H and 100.6 MHz for ^{13}C, Varian, Inc., Palo Alto, *CA*, USA,) or on a Varian VNMRS 600 spectrometer (600. MHz for ^1H and 151.6 MHz for ^{13}C, Varian, Inc., Palo Alto, *CA*, USA) in DMSO-d_6 or $CDCl_3$ solutions; δ is given in ppm referenced to the residual solvent signal. ^1H and ^{13}C NMR signals were assigned on the basis of one- and two-dimensional homo- and heteronuclear experiments (^1H–^1H COSY, ^1H–^{13}C HMBC and ^1H–^{13}C HSQC). Melting points were determined on a SRS OptiMelt MPA100 apparatus (Stanford Research Systems, Sunnyvale, California, USA), and are uncorrected. Mass spectra were recorded on a Waters Xevo G2 XS-QTo system and evaluated on the MassLynx software. Reaction progress was followed by thin-layer chromatography on commercial silica gel plates (Merck silica gel F254 on aluminum sheets, Darmstadt, Germany) using different mobile phases. For column chromatography, Kieselgel 60 (particle size 0.040–0.063 mm, VWR Chemicals, Radnor, PA, USA) was employed.

2.2. Synthesis of the appropriate nor-compounds and alkylating agents

Normorphine, norcodeine, dihydronormorphine and dihydronorcodeine were synthesized based on literature procedure, heating the parent molecule with 1-chloroethyl-chloroformate in 1,2-dichloroethane in the presence of sodium bicarbonate, then heating the attained residue in methanol. (Olofson et al., 1984)

Trifluoroacetyl-protected bromoalkylamines were obtained by stirring the mixture of the hydrobromide salt of the appropriate bromoalkylamine with triethylamine in dichloromethane (DCM) and adding trifluoroacetic acid anhydride in DCM dropwise to the mixture, while maintaining 0 °C, and then continuing stirring the mixture at room temperature overnight. (Bartole et al., 2020)

2.3. Determination of protonation constants by pH-potentiometric titrations

An ECO automatic titrator (Metrohm) with a Metrohm 6.0234.110 combined pH glass electrode was used for the potentiometric titrations. The electrode was calibrated by aqueous standard buffer solutions. Constant temperature (25±0.1 °C) was provided by a thermostated double-walled glass cell. Difference titrations were carried out in the absence (blank) and presence of ligands.

First 2 ml of 0.1 M HCl solutions were titrated with 0.1 M KOH. Constant ionic strength of 0.15 M was provided by the presence of KCl, then a ligand was added to the same volume of HCl solution and was subsequently titrated with KOH. The initial concentration of the ligands varied between 1 and 4 mM in the titrations, and at least three parallel measurements were carried out for each ligand. Non-linear parameter fitting with Origin 8 provided the protonation constants from the volume differences.

The cyanoalkyl derivatives were also titrated with the same method at a concentration of 1 mM in the presence of 10 mM β-cyclodextrin. The tenfold excess of β-cyclodextrin ensures the formation of a stable complex. The solubility of β-cyclodextrin did not allow the preparation of significantly more concentrated solutions.

2.4. Partition coefficient measurements by the shake-flask method

The distribution coefficients were calculated from the absorbance of the molecules in the aqueous phase before and after partitioning at several octanol/water phase ratios as previously reported. (Malik et al., 2024)

To ensure that the neutral form of the compounds has a dominant contribution to the distribution coefficient, the pH of the buffers was designed to be close to the log *K* value for monoprotic molecules, and close to the isoelectric point of diprotic molecules.

The pH was adjusted to values between 5.96 and 7.80 using solid NaH_2PO_4 and Na_2HPO_4. The osmolarity of 0.3 osmol/liter was achieved by adding solid NaCl. A water/octanol system with three different phase ratios per molecule was used. The distribution coefficients were calculated from the absorbance values before and after partitioning, and the mole fractions characteristic of the given pH were considered for the calculation of the partition coefficients.

2.5. Determination of complex stoichiometry using job's method

We investigated the complex formation of (**11**) and β-cyclodextrin. Solutions of the two substances with the same concentration of 0.4 mM

were prepared using pH 11.64 phosphate buffer. At this pH, the anionic form of the molecule dominates, which ensures proper solubility. Then, the solutions were mixed in different volume ratios and absorbances were measured using UV spectroscopy at the absorption maximum (λ =298 nm) of the investigated molecule. Cyclodextrin does not have significant absorption, so its higher ratio in the solution results in a decrease in the absorbance value.

2.6. Determination of complex structure and stability by NMR

To determine the structure and stability constants of the complex, ^{1}H and two-dimensional (COSY, HSQC, HMBC, ROESY) NMR spectra were recorded of compounds (**11**) and (**12**). The spectra, except for the ROESY spectra, were recorded using the 400 MHz Varian Mercury Plus instrument. The Hungarian Academy of Sciences provided assistance in recording the ROESY spectra using a 600 MHz Varian instrument. The substances were examined at pH values around 7 and 11, which were provided with a phosphate buffer prepared with D_2O. The apparent pH value of these solutions was converted to a conventional pH scale based on the Krezel relation, obtaining pH 7.5 and 11.6. (Krężel and Bal, 2004) For the ROESY spectrum, a 4 mM solution of (**12**) was prepared in both phosphate buffers in the presence of 16 mM β-cyclodextrin.

The solution series prepared to determine the complex stability contained the same amount of guest molecule (0.5 mM) and increasing amounts of β-cyclodextrin (0–24-fold). To aid dissolution, 5 V/V % deuterated methanol was added to the solutions where necessary.

The water signal was suppressed using the PRESAT method, and the methanol signal at 3.34 ppm was used as a reference for the chemical shifts. The spectra were processed by MestReNova 14.2 (Mestrelab Research, Santiago de Compostela, Spain), and the stability constants were determined using the global fit of Eq. (2) in Origin.

$$\delta^{Obs} = \delta_L + \Delta\delta \cdot \frac{[L]_T + [CyD]_T + \frac{1}{K} - \sqrt{\left([L]_T + [CyD]_T + \frac{1}{K}\right)^2 - 4 \cdot [L]_T \cdot [CyD]_T}}{2 \cdot [L]_T} \quad (2)$$

where $[L]_T$ and $[CyD]_T$ are the total concentrations of the guest molecule and β-cyclodextrin, δ_L the chemical shift observed for the nucleus under study. (Tűz et al., 2022)

2.7. Determination of complex stability by circular dichroism measurements

The various derivatives of cyclodextrins (CyD) are chiral, but they do not have a chromophore group and thus do not have a characteristic circular dichroism (CD) spectrum above 220 nm. By adding a non-chiral guest molecule with a chromophore, and if the complex structure is appropriate, the molecule becomes chirally perturbed and gives an induced CD signal. In the case of 1:1 complexes, the stability constant characteristic of the complex can be calculated by fitting a function to the saturation curve of the signal. For this, Eq. (2) described in NMR spectroscopy can be used in an analogous manner. (Kiss et al., 2019)

However, morphine and its derivatives are chiral molecules with a chromophore group and thus have their own characteristic circular dichroism spectrum. (Crone and Purdie, 1981) Therefore the resulting signal is the sum of the induced signal upon complexation and the already existing own signal of the molecule. We were curious whether the induced signal formed by the complex with β-cyclodextrin could be measured in addition to the existing signal, and if so, whether we could find a suitable trend in it for determining stability constants.

The measurements were performed using a Jasco J-815 circular dichroism spectrometer, under thermostated conditions at 25 °C. Solutions of the molecules under study were prepared at 1 mM concentration with phosphate buffers at pH 7.2 and 11.7. Increasing amounts of β-cyclodextrin were added to them to determine the stability constant (up to 8-fold excess). The circular dichroism signals were read at the absorption maximum of the compounds, thus around 282–285 nm at pH 7.2 and around 295–298 nm at pH 11.7. The change in the signal was followed and then plotted as a function of the increasing concentration of β-cyclodextrin, and the values of the stability constants were determined by fitting Eq. (2) described above. (Kiss et al., 2019)

3. Results and discussion

3.1. N-aminoalkyl-nor-derivatives

In this study, several opiate compounds were synthesized, in which the substituent of the pharmacologically important nitrogen atom in the piperidine ring of the morphinan skeleton was different from the usually employed methyl, allyl, or cyclopropylmethyl groups, namely, we substituted the nitrogen with cyanoalkyl and aminoalkyl groups. The goal of these syntheses was to synthetize compounds that could be used as haptens in the development of future vaccines against opiate compounds, and the four aminoalkyl derivatives fulfil this goal. Haptens with a free primary amine group at the end of their side-chain are able to form amide bonds with either a linker, or with a free carboxylic acid moiety in the carrier protein, which is advantageous over an ester group, because it is hydrolytically more stable.

Outside of this, new studies showed that it is possible to use molecules with similar substituents as active compounds at the opioid receptors. (Fig. 3)

Compounds with the cyanoalkyl substituents were synthetized for two reasons. First, when we were exploring the synthetic options leading to the aminoalkyl compounds, we felt that the cyano-group could be a useful synthon for the primary amine group found in the aminoalkyl molecules. In this case, after the introduction of the cyanoalkyl substituent, an appropriate reducing agent could be employed to acquire the primary amines. Different reducing agents were studied, but since the work-up phase of these reactions is usually more difficult, especially for compounds that are relatively soluble in water, while their solubility in the usual extraction solvents remain low, we decided that the alkylation reactions with N-protected amines would be more worthwhile. Still, we did not abandon the cyanoalkyl analogues, since the fact that they too are active compounds at the opioid receptors is a fact known from the literature. Physicochemical characterization of these compounds is lacking, so we hoped to achieve that as well in this work.

For the synthesis of the aminoalkyl compounds, many pathways were trialed. Beside the already mentioned methods using the reduction of the cyanoalkyl derivatives, we tried different protecting groups for the amine functionality, namely phthalimido, tert-butyloxycarbonyl (BOC), and the trifluoroacetyl group. Out of these, the trifluoroacetamide alkylating agents provided the cleanest reactions, with the easiest work-up procedures, all the while retaining a relatively high yield compared to the other two options. These compounds contain two base centers, which is relatively unique in morphinans, so we set out to establish their basicity values, and to look into their protonation schemes as well. This data will most probably be useful, because these derivatives can be used in several ways, either as haptens, or in animal

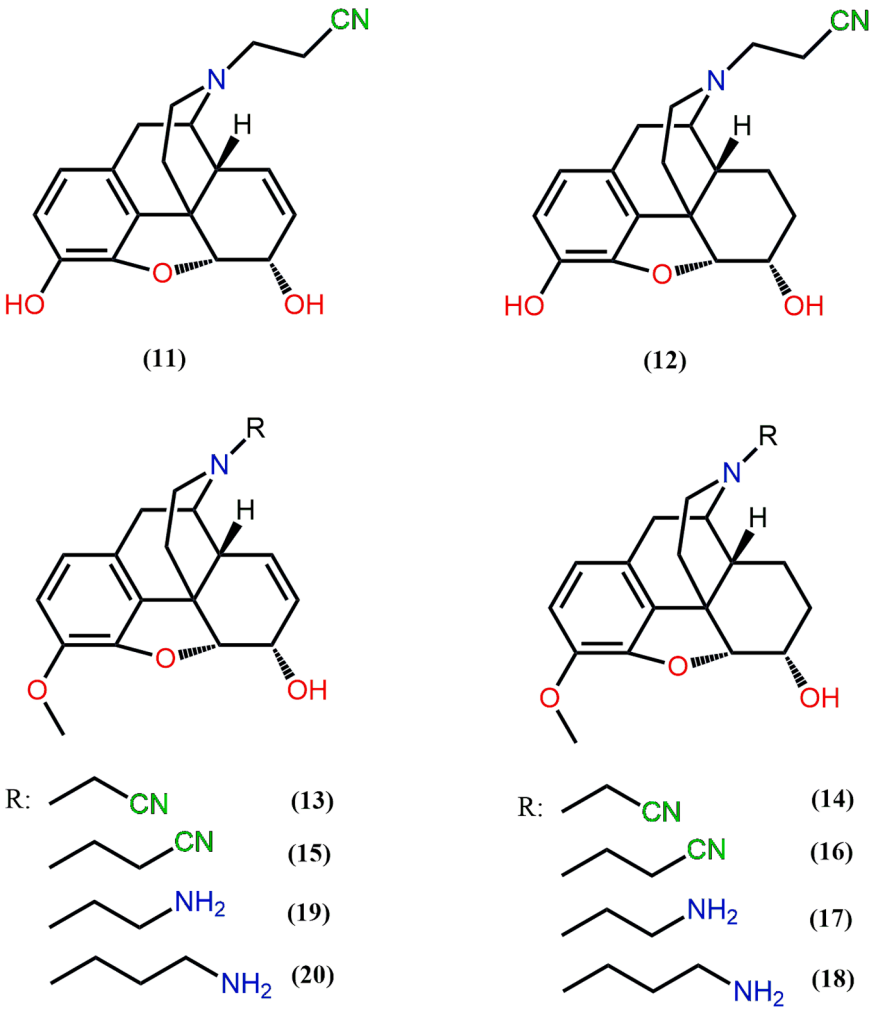

Fig. 3. Structures of the synthetized nor-opiate derivatives.

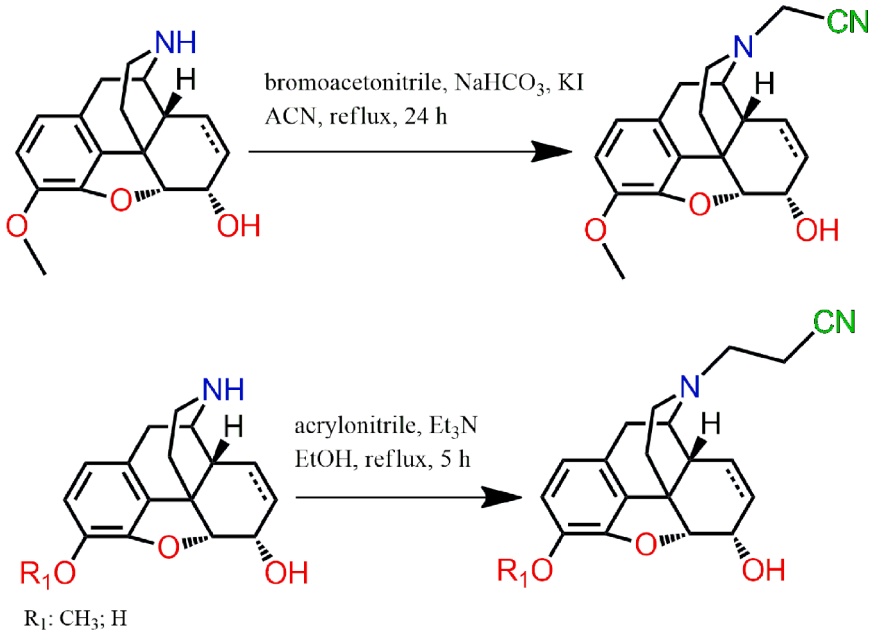

Fig. 4. Cyanoalkylation reaction scheme.

studies as potential opioid analgesics, and in either of those, physico-chemical qualities govern much that happens with a molecule in a biological setting.

3.2. Synthesis of cyanoalkyl-noropiate derivatives

3.2.1. N-cyanoethyl-derivatives

The appropriate nor-compound (1.0 mmol), acrylonitrile (2.2 mmol, 144 µl) and triethylamine (10.0 mmol, 1394 µl) were refluxed in ethanol until TLC analysis (using 9:1 cholorform:methanol as the eluent) showed that the starting compound was consumed. If needed, another 1.0 mmol of acrylonitrile was added. The ethanol was removed using a rotary evaporator, the residue taken up in distilled water, the pH value of the mixture was adjusted to 9 with aq. cc. NH_3 and extracted with chloroform (3 × 30 ml). The combined organic phases were washed with brine, and dried over anhydrous Na_2SO_4, which was then filtered off, and the solvent was removed on the rotavap. If necessary, column chromatography was performed on silica gel, using 9:1 chloroform:methanol as the eluent. (Fig. 4)

N-cyanoethylnormorphine (**11**): yield: 93 %, purity: >95 % (LC-MS); brown powder, M. p.: 209–211 °C (ethanol)

^{1}H NMR (600 MHz, DMSO-d_6) δ 6.46 (d, J = 8.1 Hz, 1H, H-2), 6.34 (d, J = 8.0 Hz, 1H, H-1), 5.54 (d, J = 9.8 Hz, 1H, H-7), 5.22 (dt, J = 9.8, 2.8 Hz, 1H, H-8), 4.68 (d, J = 6.0 Hz, 1H, H-5), 4.12 (m, 1H, H-6), 3.42 (dd, J = 6.3, 3.1 Hz, 1H, H-9), 2.82 – 2.73 (m, 2H, H-10, N—CH_2), 2.71 – 2.57 (m, 4H, H-16, N—CH_2, CH_2—CN), 2.53 (m, 1H, H-14), 2.34 – 2.27 (m, 2H, H-10, H-16), 1.97 (td, J = 12.6, 4.9 Hz, 1H, H-15), 1.63 (d, J = 12.4 Hz, 1H, H-15)

^{13}C NMR (151 MHz, DMSO-d_6) δ 146.3 (C4), 138.5 (C3), 133.6 (C7), 130.9 (C12), 128.2 (C8), 125.2 (C11), 120.1 (CN), 118.5 (C1), 116.4 (C2), 91.5 (C5), 66.4 (C6), 56.6 (C9), 50.0 (N—CH_2), 43.9 (C13), 43.3 (C16), 40.4 (C14), 35.4 (C15), 22.2 (C10), 16.5 (CH_2—CN)

HR-MS: MH^+: 325.1558 $C_{19}H_{20}N_2O_3$ (324.38)

N-cyanoethyldihydronormorphine (**12**): yield: 85 %, purity: >95 % (LC-MS); off-white powder, M. p.: 184–185 °C (ethanol)

^{1}H NMR (400 MHz, DMSO-d_6) δ 6.52 (d, J = 8.0 Hz, 1H, H-2), 6.41 (d, J = 8.0 Hz, 1H, H-1), 4.36 (d, J = 4.6 Hz, 1H, H-5), 3.80 (d, J = 9.6 Hz, 1H, H-6), 3.06 (m, 1H, H-9), 2.78 – 2.53 (m, 4H, N—CH_2, CN—CH_2), 2.44 – 2.26 (m, 2H, H-10, H-16), 2.10 (d, J = 8.1 Hz, 2H, H-14, H-16), 1.74 (m, 1H, H-15), 1.50 – 1.23 (m, 3H, H-7, H-8, H-15), 1.13 (m, 1H, H-7), 0.86 (m, 1H, H-8).

^{13}C NMR (101 MHz, DMSO-d_6) δ 146.4 (C4), 138.4 (C3), 130.5 (C12), 125.4 (C11), 120.6 (CN), 118.5 (C1), 117.1 (C2) 90.3 (C5), 66.5 (C6), 58.0 (C9), 50.5 (N—CH_2), 44.2 (C16), 42.8 (C13), 38.4 (C14), 37.5 (C15), 25.9 (C7), 22.0 (C10), 19.9 (C8), 16.8 (CH_2—CN)

HR-MS: MH^+: 327.1735 $C_{19}H_{22}N_2O_3$ (326.38)

N-cyanoethylnorcodeine (**15**): yield: 89 %, purity: >95 % (LC-MS); yellow powder, M. p.: 173–175 °C (diethyl ether)

^{1}H NMR (600 MHz, DMSO-d_6) δ 6.61 (d, J = 8.1 Hz, 1H, H-2), 6.46 (d, J = 8.0 Hz, 1H, H-1), 5.54 (dddd, J = 9.8, 3.3, 2.1, 1.3 Hz, 1H, H-7), 5.23 (dt, J = 9.7, 2.8 Hz, 1H, H-8), 4.69 (dd, J = 6.0, 1.3 Hz, 1H, H-5), 4.13 (tq, J = 5.6, 2.6 Hz, 1H, H-6), 3.72 (s, 3H, OCH_3), 3.43(m, 1H, H-9), 2.83 – 2.72 (m, 2H, H-10, N—CH_2), 2.70 – 2.60 (m, 4H, H-16, N—CH_2, CH_2—CN), 2.55 (m, 1H, H-14), 2.38 – 2.25 (m, 2H, H-10, H-16), 1.98 (td, J = 12.6, 5.0 Hz, 1H, H-15), 1.63 (m, 1H, H-15)

^{13}C NMR (151 MHz, DMSO-d_6) δ 147.2 (C4), 141.0 (C3), 133.3 (C7), 131.0 (C12), 127.7 (C8), 126.8 (C11), 120.1 (CN), 118.0 (C1), 112.8 (C2), 91.8 (C5), 66.1 (C6), 56.1 (C9), 55.7 (OCH_3), 49.8 (N—CH_2), 43.4 (C16), 41.7 (C13), 40.0 (C14), 35.1 (C15), 21.9 (C10), 16.3 (CH_2—CN)

HR-MS: MH^+: 339.1735 $C_{20}H_{22}N_2O_3$ (338.38)

N-cyanoethyldihydronorcodeine (**16**): yield: 90 %, purity: >95 % (LC-MS); faint yellow powder, M. p.: 223–224 °C (ethanol)

^{1}H NMR (600 MHz, DMSO-d_6) δ 6.69 (d, J = 8.1 Hz,1H, H-2), 6.53 (d, J = 8.2 Hz, 1H, H-1), 4.46 (d, J = 5.9 Hz, 1H, H-5), 3.83(m, 1H, H-6), 3.76 (s, 3H, OCH_3,), 3.09(m, 1H, H-9), 2.78 – 2.70 (m, 2H, N—CH_2, H-10), 2.65 – 2.60 (m, 2H, CH_2—CN), 2.59 – 2.52 (m, 2H, N—CH_2, H-16), 2.39 (dd, J = 18.5, 5.9 Hz, 1H, H-10), 2.16 – 2.07 (m, 2H, H-14, H-16), 1.79 (td, J = 12.5, 5.0 Hz, 1H, H-15), 1.49 – 1.28 (m, 3H, H-7, H-8- H-15) 1.16 (ddd, J = 16.0, 13.5, 6.9 Hz, 1H, H-7), 0.88 (ddd, J = 18.0, 13.0, 6.6 Hz, 1H, H-8)

^{13}C NMR (151 MHz, DMSO-d_6) δ 146.7 (C4), 140.7 (C3), 130.2 (C12), 127.0 (C11), 120.1 (CN), 117.8 (C1), 113.6 (C2), 90.0 (C5), 65.4 (C6), 57.2 (C9), 49.7 (N—CH_2), 43.4 (C16), 42.2 (C13), 37.9 (C14), 36.7 (C15), 25.5 (C7), 21.3 (C10), 19.1 (C8), 16.2 (CH_2—CN)

HR-MS: MH^+: 341.1889 $C_{20}H_{24}N_2O_3$ (340.38)

3.2.2. N-cyanomethyl-derivatives

The appropriate nor-compound (1.0 mmol), bromoacetonitrile (2.2 mmol, 153 µl), sodium bicarbonate (5.0 mmol, 420 mg), and potassium iodide were refluxed in acetonitrile for 24 h. After this, the inorganic salts were filtered off, the acetonitrile removed on the rotavap, and the residue was taken up in distilled water. The pH value of the mixture was adjusted to 9 with aq. cc. NH_3, and the mixture was extracted with chloroform (3 × 30 ml). The combined organic phases were washed with brine and dried over anhydrous Na_2SO_4, which was then filtered, and the solvent was removed on the rotavap. Column chromatography was performed on silica gel, with 9:1 chloroform:methanol mixture to afford the cyanomethyl derivatives.(Fig. 4)

N-cyanomethylnorcodeine (**13**): yield: 73 %, purity: >95 % (LC-MS); brown-yellow powder, M.p.: 166.1 °C (ethanol)

^{1}H NMR (600 MHz, DMSO-d_6) δ 6.63 (d, J = 8.1 Hz, 1H, H-2), 6.47 (d, J = 8.1 Hz, 1H, H-1), 5.55 (d, J = 9.4 Hz, 1H, H-7), 5.25 (dt, J = 9.8, 2.8 Hz, 1H, H-8), 4.70 (d, J = 6.0 Hz, 1H, H-5), 4.13 (td, J = 5.6, 2.6 Hz, 1H, H-6), 3.81 (d, J = 17.1 Hz, 1H, CH_2—CN), 3.73 (m, 4H, CH_2—CN, OCH_3), 3.49 (dd, J = 6.2, 3.2 Hz, 1H, H-9), 2.97 (d, J = 18.7 Hz, 1H, H-10), 2.64 (dd, J = 12.0, 4.9 Hz, 1H, H-16), 2.58 (q, J = 2.9 Hz, 1H, H-14), 2.42 (td, J = 12.3, 3.5 Hz, 1H, H-16), 2.37 (dd, J = 18.8, 6.2 Hz, 1H, H-10), 2.02 (td, J = 12.6, 5.1 Hz, 1H, H-15), 1.71 – 1.65 (m, 1H, H-15)

^{13}C NMR (151 MHz, DMSO-d_6) δ 147.2 (C4), 141.2 (C3), 133.3 (C7), 130.5 (C12), 127.6 (C8), 126.7 (C11), 118.4 (C1), 118.1 (CN), 113.3 (C2), 91.8 (C5), 66.3 (C6), 56.9 (C9), 55.8 (OCH_3), 43.5 (C16), 42.8 (C13), 42.5 (CH_2-(CN)), 40.3 (C14), 34.9 (C15), 21.8 (C10)

HR-MS: MH^+: 325.1558 $C_{19}H_{20}N_2O_3$ (324.38)

N-cyanomethyldihydronorcodeine (**14**): yield: 63 %, purity: >95 % (LC-MS), yellow powder, M.p.: 240.9 °C (ethanol)

^{1}H NMR (600 MHz, DMSO-d_6) δ 6.70 (d, J = 8.2 Hz, 1H, H-2), 6.53 (d, J = 8.1 Hz, 1H, H-1), 4.47 (d, J = 5.0 Hz, 1H, H-5), 3.82 (ddt, J = 10.2, 8.2, 5.2 Hz, 1H, H-6), 3.79 – 3.73 (m, 4H, OCH_3, CH_2—CN), 3.67 (d, J = 17.0 Hz, 1H, CH_2—CN), 3.17 (dd, J = 5.8, 2.8 Hz, 1H, H-9), 2.91 (d, J = 18.6 Hz, 1H, H-10), 2.54 (dd, J = 11.8, 4.8 Hz, 1H, H-16), 2.42 (dd, J = 18.6, 5.8 Hz, 1H, H-10), 2.26 (td, J = 12.1, 3.7 Hz, 1H, H-16), 2.14 (ddd, J = 11.8, 6.4, 2.8 Hz, 1H, H-14), 1.82 (td, J = 12.4, 5.1 Hz, 1H, H-15), 1.50 (ddd, J = 12.5, 3.7, 1.7 Hz, 1H, H-15), 1.41 – 1.27 (m, 2H, H-7, H-8), 1.20(m, 1H, H-7), 0.91 (tt, J = 11.8, 6.1 Hz, 1H, H-8)

^{13}C NMR (151 MHz, DMSO-d_6) δ 146.9 (C4), 141.0 (C3), 129.8 (C12), 126.3 (C11), 118.1 (C1), 117.9 (CN), 114.1 (C2), 89.9 (C5), 65.6 (C6), 58.1 (C9), 56.2 (OCH_3), 43.7 (C16), 42.5 (N—CH_2), 41,6 (C13), 38.2 (C14), 36.4 (C15), 25.9 (C7), 21.4 (C10), 18.9 (C8)

HR-MS: MH^+: 327.1698 $C_{19}H_{22}N_2O_3$ (326.40)

3.3. Synthesis of the aminoalkyl noropiate derivatives

3.3.1. Synthesis of the aminoethyl noropiate derivatives

The appropriate noropiate (2.0 mmol), N-(2-bromoethyl)-trifluoroacetamide (2.2 mmol, 481.7 mg), sodium bicarbonate (10.0 mmol, 840 mg), and potassium iodide were refluxed in acetonitrile for 18 h. The inorganic salts were filtered out, the acetonitrile removed on rotavap, and then the residue was taken up in saturated sodium bicarbonate solution, and extracted with chloroform (3 × 30 ml). The combined organic phases were washed with distilled water, brine, and dried over anhydrous Na_2SO_4. The chloroform was removed on the rotavap, and then column chromatography was performed on silica gel, with 9:1

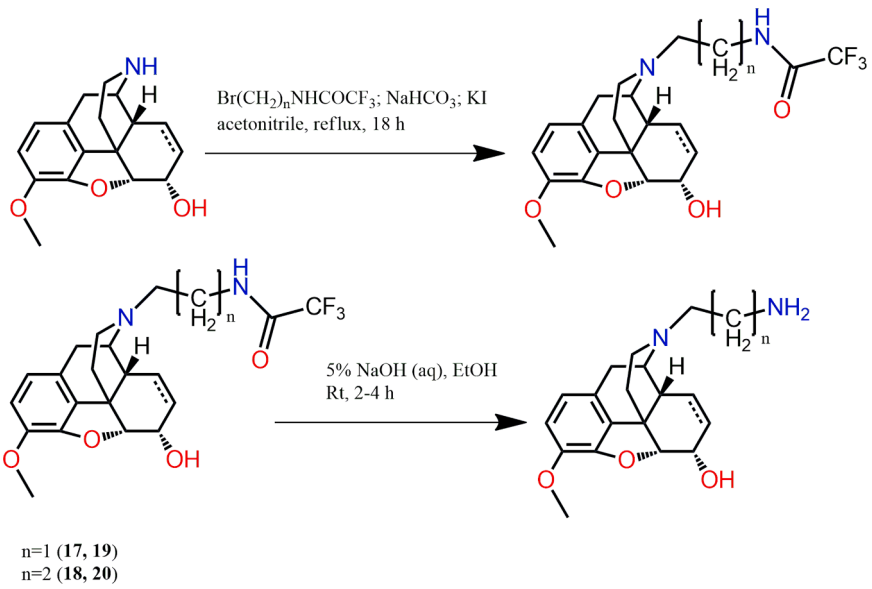

Fig. 5. Synthesis of the aminoalkyl derivatives in 2 steps.

chloroform:methanol mixture to afford the protected N-aminoethyl-noropiates as pure compounds as a brown, amorphous mass. (Fig. 5)

The trifluoroacetyl protecting group was removed by dissolving the protected amines in ethanol, adding 5 % aqueous NaOH solution, and stirring them at room temperature until the TLC analysis signaled the full consumption of the starting material (this lasted 2–4 h). After this, the solution was first concentrated, then diluted with distilled water, and extracted with chloroform (3 × 30), then the combined organic phases were washed with dist. water, brine, and dried over anhydrous Na_2SO_4, which was then filtered off. Removal of the solvent on the rotavap afforded the N-aminoethyl-noropiates as brown oils. (Fig. 5)

N-aminoethylnorcodeine (**19**): yield: 53 %, (for two steps) purity: >95 % (LC-MS), brown oil, M. p.: 210.7 (as bioxalate, ethanol)

^{1}H NMR (400 MHz, $CDCl_3$) δ 6.66 (d, J = 8.0 Hz, 1H, H-2), 6.56 (d, J = 8.2 Hz, 1H, H-1), 5.70 (d, J = 9.9 Hz, 1H, H-7), 5.28 (m, 1H, H-8), 4.89 (d, J = 6.4 Hz, 1H, H-5), 4.17 (br.s, 1H, H-6), 3.84 (s, 3H, OCH_3), 3.39 (d, J = 5.9 Hz, 1H, H-9), 2.96 (d, J = 18.5 Hz, 1H, H-10), 2.80 (s, 2H, N—CH_2), 2.71 – 2.54 (m, 3H, H-14, H-16, CH_2—NH_2), 2.51 – 2.32 (m, 2H, H-10, H-16), 2.05 (m, 1H, H-15), 1.87 (d, J = 12.4 Hz, 1H, H-15)

^{13}C NMR (101 MHz, $CDCl_3$) δ 146.8 (C4), 142.6 (C3), 133.9 (C7), 131.7 (C12), 128.9 (C8), 127.7 (C11), 119.9 (C1), 113.3 (C2), 91.9 (C5), 66.9 (C6), 58.4 (C9), 58.0 (CH_2—NH_2), 56.8 (OCH_3), 44.8 (C16), 43.99 (C13), 41.2 (C14), 39.6 (N—CH_2), 36.3 (C15), 22.7 (C10)

HR-MS: MH^+: 329.1863 $C_{19}H_{24}N_2O_3$ (328.4)

N-aminoethyldihydronorcodeine (**17**): yield: 59 %, (for two steps) purity: >95 % (LC-MS), brown oil, M.p.: 112.5 (as bitartrate, ethanol)

^{1}H NMR (400 MHz, $CDCl_3$) δ 6.71 (d, J = 8.3 Hz, 1H, H-2), 6.62 (d, J = 8.1 Hz, 1H, H-1), 4.59 (d, J = 5.2 Hz, 1H, H-5), 4.02 (br.s, 1H, H-6), 3.87 (s, 3H, OCH_3), 3.09 (d, J = 5.3 Hz, 1H, H-9), 2.91 (d, J = 18.3 Hz, 1H, H-10), 2.76 (s, 2H, N—CH_2), 2.56 (d, J = 14.0 Hz, 2H, CH_2—NH_2), 2.48 – 2.41 (dd, J = 18.7, 5.8 Hz, 1H, H-10), 2.31 – 2.15 (m, 2H, H-16, H-14), 1.85 (m, 1H, H-15), 1.68 (d, J = 12.2 Hz, 1H, H-15), 1.61 – 1.35 (m, 2H, H-7), 1.25 (m, 1H, H-8), 1.11 (m, 1H, H-8).

^{13}C NMR (101 MHz, $CDCl_3$) δ 146.6 (C4), 142.0 (C3), 130.9 (C12), 127.5 (C11), 119.6 (C1), 113.6 (C2), 90.9 (C5), 67.72 (C6,) 59.2 (C9), 58.2 (CH_2—NH_2), 56.8 (OCH_3), 45.1 (C16), 43.2 (C13), 40.8 (C14), 39.7 (N—CH_2), 37.9 (C15), 27.57 (C7), 22.2 (C10), 19.7 (C8).

HR-MS: MH^+: 331.2016 $C_{19}H_{26}N_2O_3$ (330.4)

3.3.2. *Synthesis of the aminopropyl noropiate derivatives*

The appropriate noropiate (2.0 mmol), N-(3-bromopropyl)-trifluoroacetamide (2.2 mmol, 514.8 mg), sodium bicarbonate (10.0 mmol, 840 mg), and potassium iodide were refluxed in acetonitrile for 18 h. The inorganic salts were filtered out, the acetonitrile removed on rotavap, and then the residue was taken up in saturated sodium bicarbonate solution and extracted with chloroform (3 × 30 ml). The combined organic phases were washed with distilled water, brine, and dried over anhydrous Na_2SO_4. The chloroform was removed on the rotavap, and then column chromatography was performed on silica gel, with 9:1 chloroform:methanol mixture to afford the protected N-aminopropyl-noropiates as pure compounds as a brown, amorphous mass. (Fig. 5)

The trifluoroacetyl protecting group was removed by dissolving the protected amines in ethanol, adding 5 % aqueous NaOH solution, and stirring them at room temperature until the TLC analysis signaled the full consumption of the starting material (this lasted 2–4 h). After this, the solution was first concentrated, then diluted with distilled water, and extracted with chloroform (3 × 30), then the combined organic phases were washed with dist. water, brine, and dried over anhydrous Na_2SO_4, which was then filtered off. Removal of the solvent on the rotavap afforded the N-aminopropyl-noropiates as brown oils. (Fig. 5)

N-aminopropylnorcodeine (**20**): yield: 53.6 %, (for two steps) purity: >95 % (LC-MS), brown oil, M. p.: 215.6 °C (as bioxalate salt, ^{1}H NMR (400 MHz, $CDCl_3$) δ 6.65 (d, J = 8.2 Hz, 1H, H-2), 6.55 (d, J = 8.3 Hz, 1H, H-1), 5.70 (d, J = 9.9 Hz, 1H, H-7), 5.28 (d, J = 9.9 Hz, 1H, H-8), 4.88 (d, J = 6.5 Hz, 1H, H-5), 4.17 (br.s, 1H, H-6), 3.84 (s, 3H, OCH_3), 3.45 (t, J = 4.2 Hz, 1H, H-9), 2.97 (d, J = 18.5 Hz, 1H, H-10), 2.86 (s, 2H, N—CH_2), 2.71 (m, 1H, H-16), 2.62 (m, 3H, CH_2—NH_2, H-14), 2.57 – 2.42 (m, 4H, CH_2—NH_2, H-16), 2.34 (dt, J = 18.0, 9.9 Hz, 2H, H-16), 2.02 (d, J = 14.4 Hz, 1H, H-15), 1.87 (d, J = 12.6 Hz, 1H, H-15), 1.69 (d, J = 7.2 Hz, 2H, N—CH_2—$\underline{CH_2}$—CH_2—NH_2)

^{13}C NMR (101 MHz, $CDCl_3$) δ 146.8 (C4), 142.7 (C3), 133.9 (C7), 131.6 (C12), 128.8 (C8), 127.6 (C11), 119.9 (C1), 113.4 (C2), 91.8 (C5), 66.9 (C6), 57.7 (C9), 56.8 (OCH_3), 53.8 (CH_2—NH_2), 45.1 (C16), 44.0 (C13), 41.3 (C14) 39.4 (N—CH_2), 36.3 (C15), 30.3 (N—CH_2—$\underline{CH_2}$—CH_2—NH_2), 21.7 (C10).

HR-MS: MH^+: 343.2026 $C_{20}H_{26}N_2O_3$ (342.4)

N-aminopropyldihydronorcodeine (**18**): yield: 40 %, (for two steps) purity: >95 % (LC-MS), brown oil, M. p.: 161.2 °C) (as bitartrate, ethanol)

^{1}H NMR (400 MHz, $CDCl_3$) δ 6.71 (d, J = 8.2 Hz, 1H, H-2), 6.61 (d, J = 8.2 Hz, 1H, H-1), 4.59 (d, J = 5.2 Hz, 1H, H-5), 4.02 (s, 1H, H-6), 3.87 (s, 3H, OCH_3), 3.16 (m, 1H, H-9), 2.92 (d, J = 18.3 Hz, 1H, H-10), 2.80 (s, 2H, N—CH_2), 2.58 (dd, J = 19.3, 10.6 Hz, 3H, H-16, CH_2—NH_2), 2.39 (dd, J = 18.3, 5.8 Hz, 1H, H-10), 2.20 (m, J = 12.6 Hz, 2H, H-16, H-14),

1.84 (m, 1H, H-15), 1.74 – 1.59 (m, 3H, H-15, N—CH_2—CH_2—CH_2—NH_2), 1.60 – 1.38 (m, 2H, H-7, H-8), 1.11 (m, 1H, H-8).

^{13}C NMR (101 MHz, $CDCl_3$) δ 146.0 (C4), 141.4 (C3), 130.3 (C12), 126.8 (C11), 118.9 (C1), 112.9 (C2), 90.3 (C5), 67.1 (C6), 57.8 (C9), 56.2 (OCH_3), 53.0 (CH_2—NH_2), 44.8 (C16), 42.6 (C13), 40.8 (N—CH_2), 40.32 (C14), 37.3 (C15), 30.6 (N—CH_2—CH_2—CH_2—NH_2), 26.9 (C7), 20.6 (C10), 19.1 (C8)

HR-MS: MH^+: 345.2185, $C_{22}H_{26}N_2O_3$ (344.4)

3.4. Characterization of acid-base properties

The O-methyl opioid N-cyanomethyl compounds (**13–16**) can only be protonated on their amino site. However, (**11**) and (**12**) can be protonated on their phenolate sites as well, thus in solution they exist in four microscopic protonation forms (microspecies) (Fig. 6), including the anionic, cationic, zwitterionic, and non-charged ones. (Mazák et al., 2019)

K_1 and K_2 are the stepwise macroconstants, k^N, k^O, k^O_N and k^N_O are the microconstants, indices O and N designate phenolate and tertiary amino site oxygen and nitrogen atoms, respectively.

Superscripts of the microscopic protonation constants indicate the group protonating in the given microequilibrium process, whereas the subscript (if any) stands for the group holding proton during the process.

The microscopic protonation pathways of the aminoalkyl compounds (**17–20**), exemplified in Fig. 7 on (**18**) is especially interesting, as these compounds possess two aliphatic amino groups, a primary and a tertiary one, connected by two and three carbon atoms, respectively.

In the case of diprotic molecules, the determination of microscopic constants is also necessary to characterize the acid-base properties of individual functional groups. One possibility to obtain microconstants is to use the macroscopic constant of a model compound that is simpler than the molecule under study as a microconstant of the structurally appropriate microspecies. The other possibility is to use the interactivity parameter between two groups already known in a small molecule for the same functional groups of a larger molecule.

3.4.1. Determination of protonation macroconstants by pH-potentiometric titrations

The logarithm values of protonation macroconstants (K_1 and K_2) obtained by the potentiometric titrations are summarized in Table 1.

3.4.2. Determination of protonation microconstants by the deductive method

For this calculation the knowledge of macroconstants (from the previous potentiometric titrations) is necessary. In the case of molecules with two protonating groups the relationships between the macroconstants and the microconstants can be seen in Eqs. (3) and (4).

$$K_1 = k^{Np} + k^{Nt} \tag{3}$$

$$K_1 K_2 = k^{Nt} k^{Np}_{Nt} = k^{Np} k^{Nt}_{Np} \tag{4}$$

For the diprotic cyanoalkyl compounds (**11, 12**), the protonation microconstants can be determined by using the macroconstants of monoprotic model molecules with similar structures (Mazák et al., 2009). We had access to O-methyl derivatives (**15, 16**) as model compounds, which had only one protonating group, the tertiary amino group. This method assumes that the effect of the modified group on the basicity of other groups is equivalent to that of the protonated form of the original group (Pálla et al., 2023). Thus, the K macroconstants of the O-methyl derivatives can be used as the k^N_O microconstants of the morphine derivatives as can be seen in Fig. 6.

However, the macroconstants of the methoxy compounds are very close to the K_2 constants of the morphine derivatives, so it can be stated that the dominant protonation pathway leads through the non-charged microspecies. Accordingly, the K_1 and K_2 constants of the morphine derivatives can practically be assigned to the protonation of the phenolate and the amino groups, respectively. The concentration of the zwitterion in the minor protonation pathway is several orders of magnitude smaller than that of the non-charged microspecies. The determination of a microconstant related to the minor protonation pathway is more valuable, since conditions of the accurate calculation of the other microconstants are then better (Mazák and Noszál, 2016). However, in our case the necessary N-methyl model compounds were not available.

The effect of the introduction of the cyanoalkyl substituent on the macroconstants can be investigated in comparison with the constants of the methyl-substituted nor-derivatives of the corresponding structure, whose protonation constants have been determined previously in our research group. (Mazák et al., 2019) The introduction of the cyanoalkyl substituent significantly reduces the basicity of the amino group. On average, this effect is 5.1 and 2.2 log units at a distance of one and two carbon atoms, respectively. Thus, the methylene group introduced into the connecting bridge reduced the electron-withdrawing effect exerted by the cyano group by nearly three log units. In contrast, the basicity of

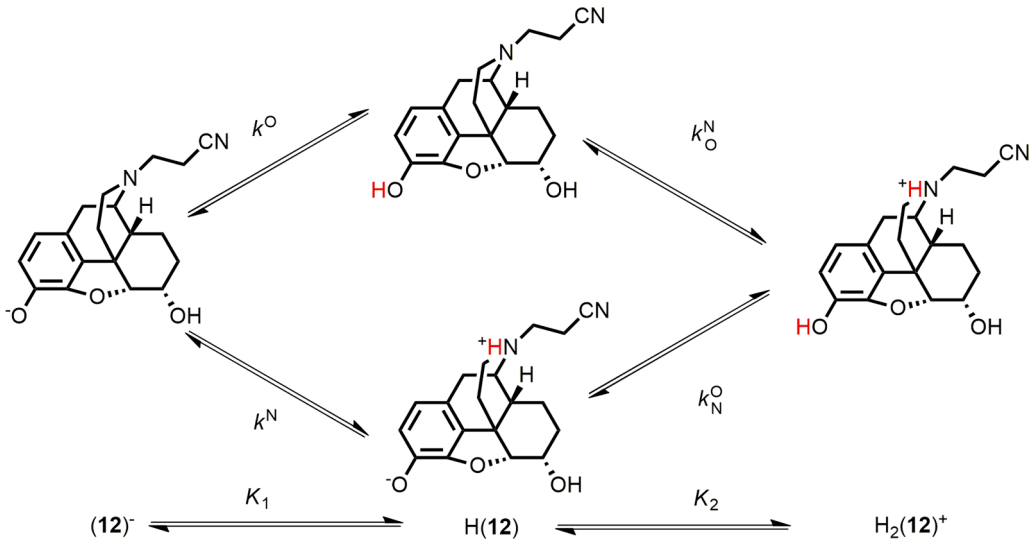

Fig. 6. The protonation equilibria of (**12**) in terms of macroscopic (K_1, K_2) and microscopic (k^N, k^O, k^O_N and k^N_O) protonation constants.

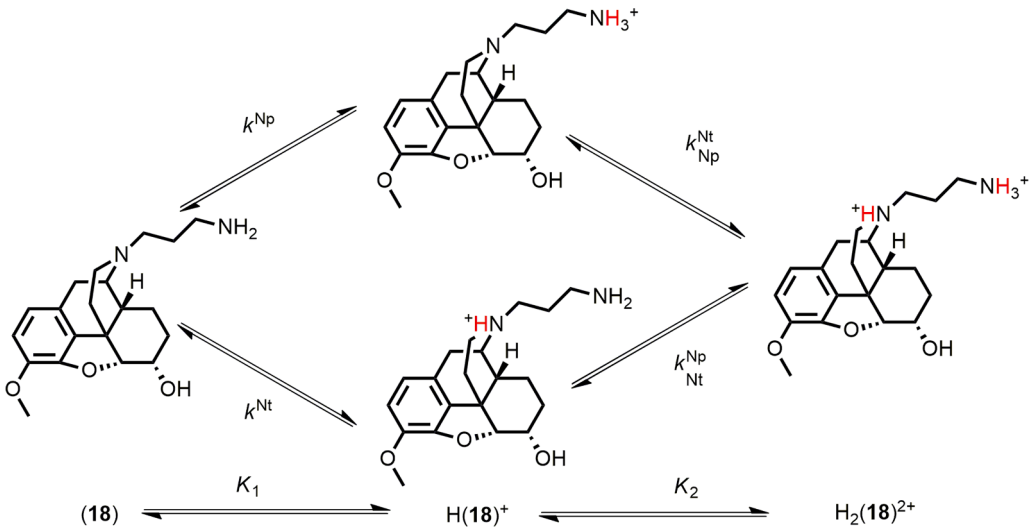

Fig. 7. Microspeciation scheme of the aminoalkyl compound (**18**). Np and Nt stand for the primary and the tertiary amino groups, respectively.

Table 1
Logarithms of the protonation macroconstants of the investigated opioid ligands. The standard deviations of the protonation macroconstants are in parenthesis.

Compound	log K_1	log K_2	Compound	log K
(11)	9.28 (0.05)	5.84 (0.05)	**(13)**	3.20 (0.05)
(12)	9.51 (0.03)	6.53 (0.02)	**(14)**	3.54 (0.02)
(17)	9.55 (0.01)	5.87 (0.03)	**(15)**	5.85 (0.05)
(18)	10.15 (0.05)	7.55 (0.02)	**(16)**	6.55 (0.01)
(19)	9.51 (0.03)	5.12 (0.01)		
(20)	10.10 (0.03)	6.96 (0.03)		

the phenolate group located further away in space was only slightly affected by the substitution, reduced by an average of 0.24 log units.

The saturation of the C7-C8 double bond increases the electron density in the molecule, and thus the basicity of the amino and phenolate groups. It increases the basicity with an average of 0.70 logarithm units of the amino group of cyanoethyl derivatives and with 0.23 units of the phenolate group.

The species-specific basicity description of the four aminoalkyl compounds (**17–20**) is especially interesting and challenging (Fig. 7). Here the primary and tertiary amino groups of similar basicity are connected by two and three carbon atoms, respectively.

In this case the only possibility for the determination of their basicity is using the pair-interactivity parameter (log E), which serves as an indicator to what extent the protonation at one basic site decreases the basicity of the other site. Its actual form for the primary and tertiary amino groups can be written as:

$$\log E = \log k^{Np} - \log k^{Np}_{Nt} = \log k^{Nt} - \log k^{Nt}_{Np} \quad (5)$$

The pair-interactivity parameter is a relatively invariant quantity. It is perturbed to a lesser extent by the protonation and the concomitant electron withdrawing effects of other groups than the microconstants themselves. The pair-interactivity parameter pertaining to the same molecular fragment and analogous pair of functional groups can therefore be transferred from small molecules to appropriate moieties of large molecules. (Mazák and Noszál, 2016)

To this end, we used the protonation constants of symmetrical primary and tertiary diamines with a distance of two and three carbon atoms, as measured experimentally in the literature (de Robertis et al., 2001; Xiao et al., 2018) and based on our own measurements and then calculated the interactivity parameters from them. The structures of the model compounds used are presented in Fig. 8.

For the interactivity parameter between primary and tertiary amino groups characteristic of the aminoethyl side chain, we used the arithmetic mean of the interactivity parameters calculated from the macroconstants of 1,2-ethanediamine and N,N,N',N'-tetramethyl-1,2-ethanediamine, as symmetrical primary and tertiary diamines, taking into account the data of our own measurements in the case of the available compounds. In a similar way, in the case of our compounds

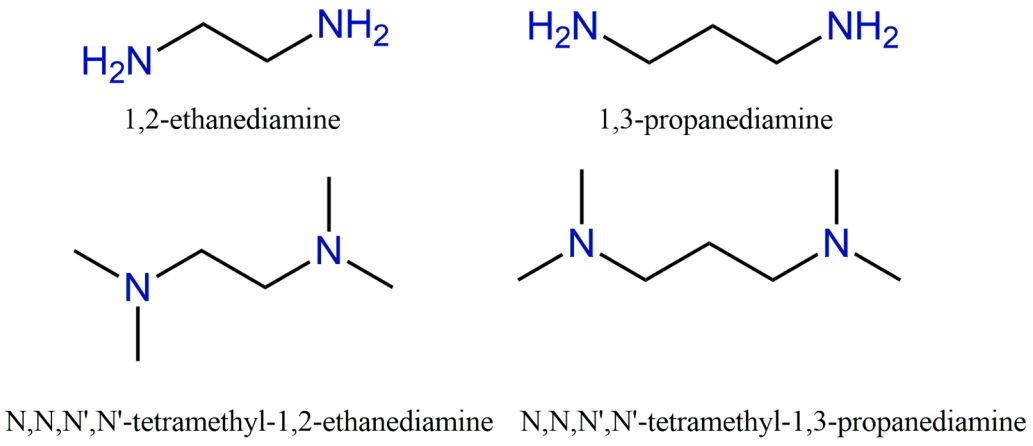

Fig. 8. Structure of symmetrical primary and tertiary diamines used as model compounds.

Table 2
The experimental interactivity parameters of model compounds used to calculate the interactivity parameter for aminoalkyl derivatives.

Compound	log *E*		
	our measurement	literature data	arithmetic mean
1,2-ethanediamine	2.32	2.49	2.56
tetramethyl-1,2-ethanediamine	–	2.79	
1,3-propanediamine	1.28	1.38	1.44
tetramethyl-1,3-propanediamine	–	1.61	

Table 3
Logarithm of protonation microconstants of aminoalkyl derivatives.

Compound	log k^{Np}	log k^{Nt}	log $k^{Nt}{}_{Np}$	log $k^{Np}{}_{Nt}$	log k_z
(**17**)	9.51	8.47	5.91	6.95	1.04
(**18**)	10.12	9.02	7.58	8.68	1.10
(**19**)	9.50	7.69	5.13	6.94	1.81
(**20**)	10.09	8.41	6.97	8.65	1.68

with aminopropyl side chains, we applied the average of the interactivity parameters of 1,3-propanediamine and N,N,N',N'-tetramethyl-1,3-propanediamine to our asymmetric amines.

The experimental interactivity parameters measured by us and collected from the literature are summarized in Table 2.

In the knowledge of the interactivity parameter, we solved the system of linear equations consisting of Eqs. (3), (4) and (5) with the help of the Wolfram Alpha computer program. *(Accessed on 19 March 2024)* to obtain k^{Np} and k^{Nt}. (Wolframalpha n.d)

Since according to several prediction computer programs, the basicity of the primary amino group at the end of the side chain significantly exceeds that of the tertiary one, we assigned the larger of the obtained microconstants to the primary and the smaller to the tertiary amino group. The calculated microconstant values are presented in Table 3, which also contains the pH-independent (but solvent-dependent) log k_z parameter ($k_z = k^{Np}/k^{Nt}$).

Based on the results obtained, the dominant protonation pathway leads through the protonated form on the primary amino group shown in Fig. 7. The positive charge formed by the protonation of the primary amino group has an electron-withdrawing effect on the non-bonding electron pair of the tertiary amino group. This explains why, compared to the value of unsubstituted dihydrocodeine (log *K* 8.76), the basicity of the tertiary amine of the N-aminopropyl derivative (**18**) decreased by 1.18, and that of the N-aminoethyl derivative (**17**) by 2.85 logarithm units. It is also clear from the two values that the electron-withdrawing effect is much more significant through the ethylene bridge than in the case of the propylene bridge, which is one carbon atom longer. The same tendency could be observed for the codeine derivatives, the basicity of the tertiary amine of (**20**) and (**19**) are 1.25 and 3.09 logarithm units lower than in codeine (log *K* 8.22).

Like in the cyanoalkyl derivatives, the saturation of the C7-C8 double bond mainly affects the nearby tertiary amino group. The increments in its basicity are 0.78 and 0.61 logarithm units for the N-aminoethyl and N-aminopropyl derivative, respectively. This saturation barely affects the more remote primary amino group.

The microconstants can be used to determine the mole fraction of the microspecies as a function of pH. The distribution of the variously protonated forms calculated using the microconstants is shown in Fig. 9 and Fig. S33 for (**17**) and (**19**), respectively. The pH-independent concentration ratio of the protonation isomers is 11.0 and 64.6 for the two compounds, respectively. Thus, in the case of the dihydrocodeine derivatives (**17**) and (**18**), the concentrations of the two protonation isomers are more comparable, as can be observed in Fig. 9. These mole fraction values are also essential in constructing lipophilicity profiles.

3.5. Characterization of lipophilicity

Various methods have been outlined for the direct determination of the distribution coefficient, but the shake-flask method remains the gold

Table 4
Logarithm of the partition coefficients of the non-charged species and standard deviation of the measured values.

compound	log *p*
(**11**)	0.73 (0.02)
(**12**)	0.81 (0.05)
(**15**)	0.90 (0.03)
(**16**)	1.09 (0.05)

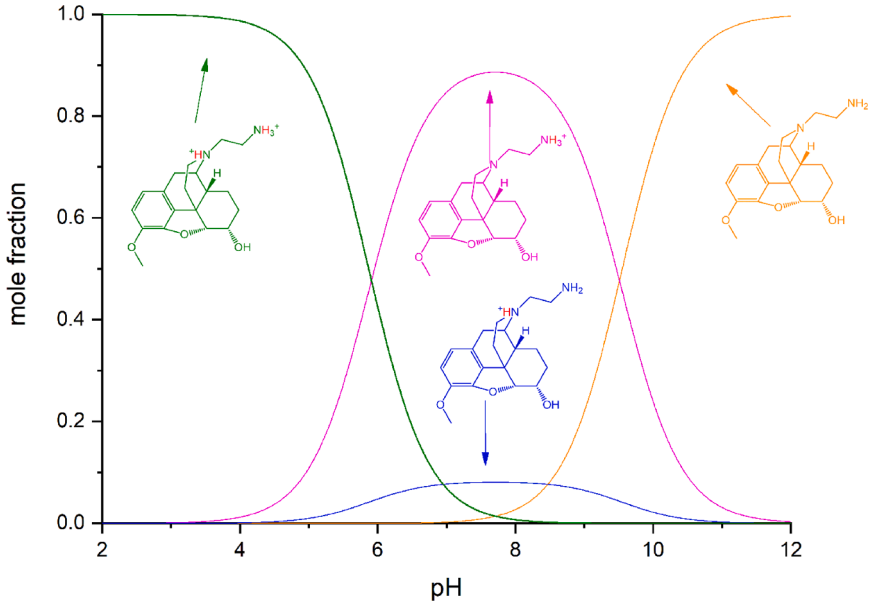

Fig. 9. The pH-dependent distribution of protonation forms of (**17**).

standard. Due to the limited solubility of the neutral form of the O-methyl cyanoethyl derivatives (**15**) and (**16**), distribution coefficients could not be determined at high enough pH values where this form is completely dominant. Nevertheless, in the knowledge of the *K* protonation constant and the pH of the solution, the log *P* values could be calculated for the more lipophilic neutral form using Eq. (1) at lower pH values where the cationic form is not completely dominant.

The partition coefficient of the non-charged form (p_N) of the cyanoethyl phenol derivatives (**11**) and (**12**) can be determined by measuring *D* values near their isoelectric point. Table 4 shows the logarithms of the partition coefficients of the non-charged species for the investigated cyanoalkyl derivatives.

The values confirm the expected result that O-methyl derivatives etherified at the hydroxyl group are more lipophilic than the corresponding phenol analogues. For derivatives with an unsaturated bond, this difference is 0.17 logarithm units, and for dihydro compounds it is slightly larger, 0.28 units. Furthermore, a tendency can be observed that the lipophilicity of dihydro derivatives saturated at the C7-C8 double bond is higher than that of the unsaturated analogues. In the case of the phenol analogues, the log *p* value increment upon saturation of this bond is 0.08, while in the case of O-methyl derivatives it is 0.19 logarithm units. Comparing the partition coefficients of the cyanoethyl derivatives to the parent compounds (Mazák et al., 2019) reveals that the introduction of the polar cyanoalkyl side chain reduces the lipophilicity of the molecules on average by 0.25 logarithm units.

3.6. Complex formation with β-cyclodextrin

Determination of complex stoichiometry using Job's method

The Job-diagram is shown in Fig. S32, from which it can be established that it has a minimum at a mole fraction value of 0.5. This confirms that (**11**) forms a 1:1 complex with β -cyclodextrin. We have already observed the formation of 1:1 complexes between other opioid molecules with β -cyclodextrin. (Tűz et al., 2022)

Effect of complex formation on the acid-base properties of the molecules

We investigated how the acid-base properties of the molecules change upon complexation with β-cyclodextrin. This was done by comparing the protonation constants measured without and in a tenfold excess of β-cyclodextrin. The results are summarized in Table 5.

For the log K_2 values assigned to the amino group of the cyanoethyl derivatives, we observed a decrease of 0.6–0.8 logarithm units in each case, while the log K_1 values showed only a minimal decrease of 0.1–0.2 units. This difference already indicates that the tested compounds enter the inner cavity of the β-cyclodextrin molecule with their halves containing the amino group.

In the β-cyclodextrin complex, the amino group is protonated only at higher H^+concentration, which results in a decrease of the log *K* value. The almost negligible change in the basicity of the phenolic hydroxyl group suggests that this part of the molecule does not participate in the complex formation, and thus the presence of β-cyclodextrin does not affect its protonation process.

We also performed measurements with N-cyanomethyl compounds, but the low initial log *K* values, between 3–3.5, decreased to such an extent after complexation that they could not be determined under the applied experimental conditions, since potentiometry is generally not suitable for determining protonation constants below pH 3.

Table 5
Logarithm and standard deviation of protonation macroconstants without and in the tenfold excess of β-cyclodextrin.

	without β-cyclodextrin		with β-cyclodextrin	
compound	log K_1	log K_2	log K_1	log K_2
(**11**)	9.28 (0.05)	5.84 (0.05)	9.17 (0.03)	5.20 (0.03)
(**12**)	9.51 (0.03)	6.53 (0.02)	9.28 (0.05)	5.81 (0.05)
	log *K*		**log *K***	
(**15**)	5.85 (0.05)		5.18 (0.05)	
(**16**)	6.55 (0.01)		5.67 (0.05)	

Determination of complex structure by NMR spectroscopy

The structure of the β-cyclodextrin complex with (**12**) was determined based on ROESY spectra, which provide information about the intermolecular interactions between the cyanoethyl guest molecule and the cyclodextrin, in case they are located within a distance of 5 Å. (Tűz et al., 2022)

Fig. 10 depicts a part of the ^{1}H NMR spectrum of β-cyclodextrin on the f1-axis and the guest molecule (**12**) on the f2-axis at pH 11.6. The hydrogen atoms between the 1.8–3.2 ppm chemical shift values (from left to right: H9, H10, H16, the four hydrogen atoms of the two methylene groups of the side chain, H14 and H16, and H15) interact with both the H3 atom of β-cyclodextrin at 3.95 ppm and the H5 atom at 3.84 ppm. Furthermore, an interaction with the H6 proton located along the smaller cavity opening of β-cyclodextrin can be observed in the overlapping part containing the H10, H16, and the hydrogen signals of the side chain. However, the H7 and H8 atoms around 1.5–1.6 ppm are only in close proximity to the H3 hydrogen located towards the wider cavity opening of the β-cyclodextrin.

Fig. 11 shows the region of aromatic hydrogen atoms. The aromatic H2 and H1 atoms only interact with the H3 atom located towards the wider cavity opening of the β-cyclodextrin. The atoms of the guest molecule do not interact with the 3.55–3.35 ppm signals of H1 and H2 located on the outside of the cyclodextrin ring.

The spectrum at pH 7.5 showed no significant differences, indicating the protonation state of the phenolate group does not influence the structure of the complex. These observations concur with the model previously established and published by our research group for other opioid derivatives, namely that the side chain and the region surrounding the amino group are responsible for fitting into the β-cyclodextrin cavity. (Tűz et al., 2022) This fitting is modeled in Fig. 12.

Determination of complex stability constants by NMR spectroscopy

The chemical shift values examined with increasing concentrations of β-cyclodextrin showed a correlation with the model established based on the ROESY spectrum. Accordingly, the largest changes were measured in the chemical shift values of the hydrogen atoms surrounding the amino group and attached to the carbon atoms of the side chain. This is demonstrated by the spectrum detail shown in Fig. S34, where it can be observed how the chemical shift of the hydrogen signals was followed. Plotting the chemical shift changes we obtained the curve shown in Fig. 13, to which we fitted Eq. (2) to calculate the stability constant.

The logarithms of the stability constant values determined in this way are summarized in Table 6. In the case of (**11**), we obtained approximately the same value for the stability of the complex formed at pH 7.5 and pH 11.6, with which the value measured for (**12**) at pH 7.5 can also be compared. However, the stability of this latter compound at alkaline pH was significantly lower, which can be paralleled by the fact that the measurable chemical shift change was much smaller for both the protons of the compound and the protons of β-cyclodextrin.

Determination of complex stability constants by circular dichroism spectroscopy

We noticed an interesting phenomenon in the spectra of cyanoethyl derivatives recorded at different pH values, which is shown in Fig. 14.

In the case of the phenolic hydroxyl group, the only chromophore group of our molecules, it is not surprising that with the increase in pH, and thus with the increase in the proportion of deprotonated species, the absorption maximum shifts towards a higher wavelength, from 282–285 nm to 295–297 nm. However, while at near-neutral pH, a negative CD curve can be observed together with the absorption maximum, at alkaline pH a sign change occurs, and we see a positive CD curve in the

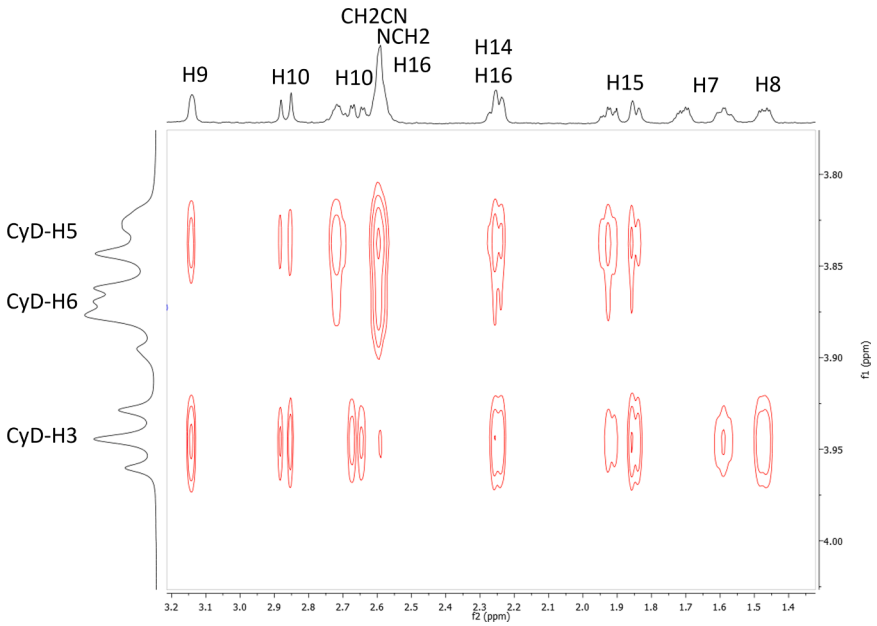

Fig. 10. ROESY spectrum of (**12**) and β-cyclodextrin in the chemical shift range of hydrogen atoms around the amino group and in the side chain.

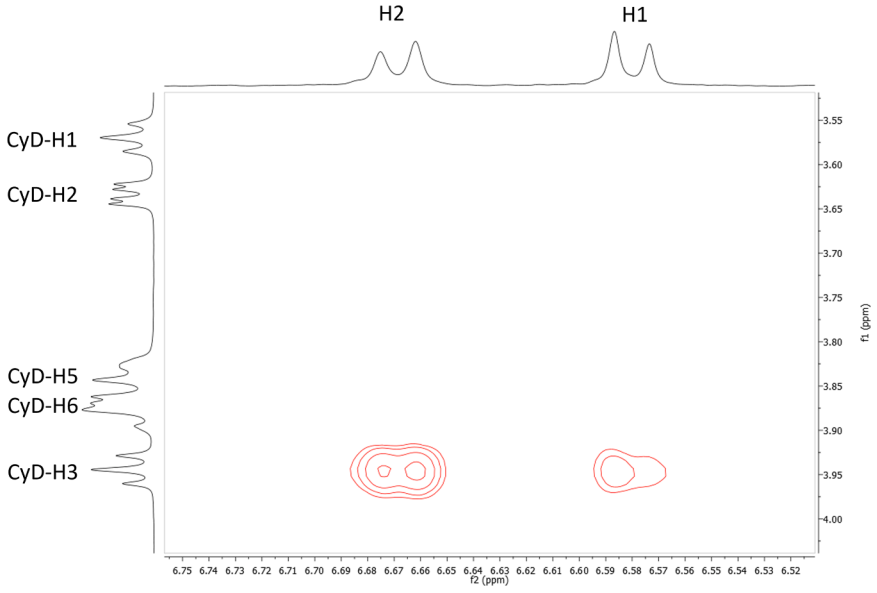

Fig. 11. ROESY spectrum of (**12**) and β-cyclodextrin in the region of aromatic hydrogen atoms.

higher wavelength range corresponding to the shifted absorbance values.

Searching the literature, we found that this phenomenon has already been described for morphine and other derivatives unsubstituted on the phenolic hydroxyl group, such as nalorphine. (Crone and Purdie, 1981) As the pH increases, and thus the ionization of the phenolic hydroxyl group increases, the positive Cotton effect gradually appears at about 300 nm, at the expense of the negative band around 285 nm. As a result, the negative band is no longer observed at high pH.

X-ray diffraction studies of morphine have shown that the aromatic ring is forced out of the plane by steric strain within the molecule. As a result, carbon atom 12 deviates from the plane of the aromatic "A" ring by 0.03 Å. The delocalization of the negative charge on the oxygen due to deprotonation aligns the atoms of the aromatic ring in a plane, thus changing the spatial arrangement of the substituents. Based on the quadrant (four-sector) rule, the sign change is caused by the displacement of the substituents from one sector to another, mainly in the case of carbon atoms 5 and 13. (Bye, 1976)

The logarithm values of the stability constants determined by fitting Eq. (4) are given in Table 6, together with the results measured by NMR. The difference seen at alkaline pH in the case of (**11**) can be explained by the phenomenon presented above. In the case of (**12**), the dihydronormorphine derivative, only a minimal, 1–2 %, induced CD signal change was measured under the influence of β-cyclodextrin, from which it was not possible to calculate a stability constant with this method.

4. Conclusions

In this study we synthetized several new N-noropiate derivatives, which could be used as haptens in the fight against opioid use disorder, or as new, potentially less harmful opioid analgesics, and determined the protonation constants and partition coefficients of N-cyano- and N-

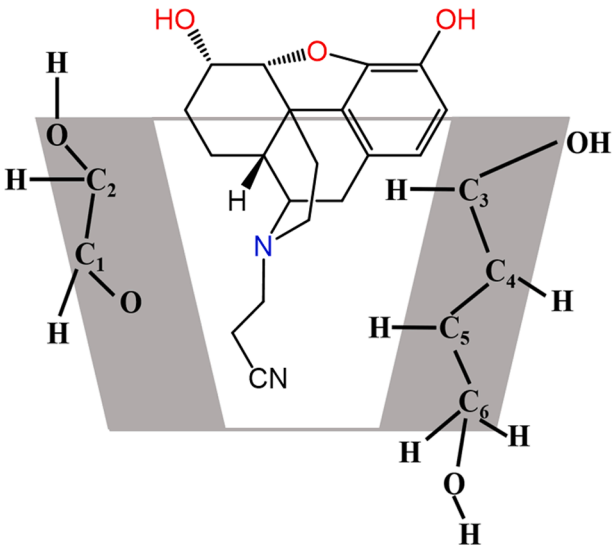

Fig. 12. Insertion model of (**12**) into the β-cyclodextrin ring based on the ROESY spectrum.

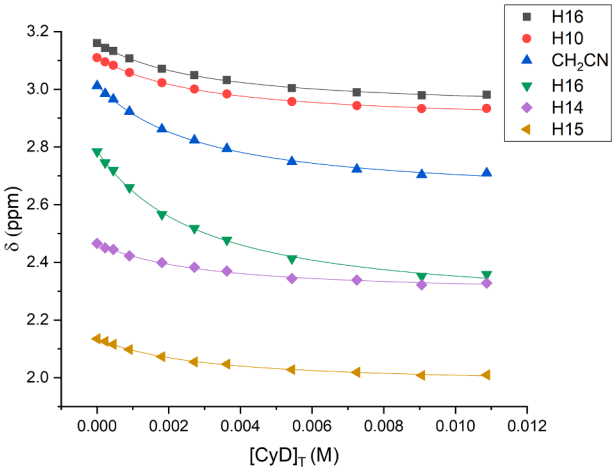

Fig. 13. Change in chemical shift values of (**12**) as a function of β-CyD concentration in a solution at pH 11.6.

Table 6
Comparison of logarithm values of stability constants measured by the two methods.

	NMR		CD	
Compound	**pH 7.5**	**pH 11.6**	**pH 7.2**	**pH 11.7**
(**11**)	3.08	3.20	3.12	2.51
(**12**)	3.05	2.59	–	–

aminoalkyl-normorphine derivatives. After comparing these quantities, we established relationships between the structure and some physicochemical parameters. Compared to unsubstituted derivatives with the appropriate structure, the introduction of the electron-withdrawing cyano group significantly reduced the basicity of the amino group. The primary amino group introduced into the side chain also reduced the basicity of the tertiary amino group of the backbone. In the case of both functional groups, it was characteristic that the basicity-modifying effect decreased with the increase in the length of the connecting side chain. The introduction of the polar cyano group also reduced the lipophilicity of the molecules. The in-depth understanding of the basicity of the various amino groups in the side chain facilitates the planning and

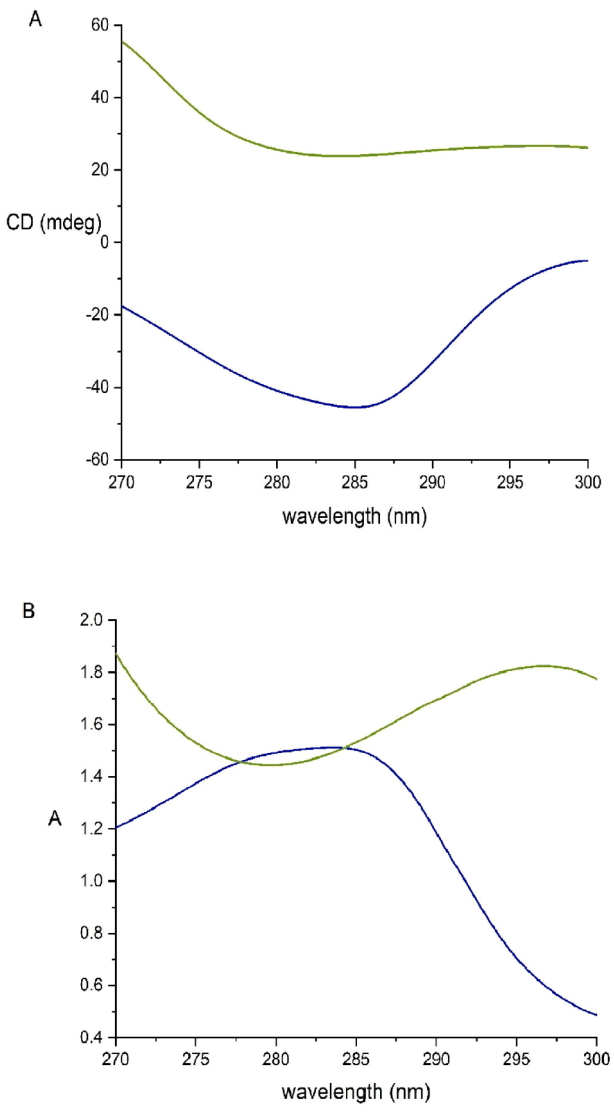

Fig. 14. Detail of the CD and UV–VIS spectra of (**11**). The spectrum recorded at pH 7.2 is shown in blue, and the spectrum recorded at pH 11.7 in green.

optimizing of further synthetic reactions to couple these haptens to carrier molecules, and possibly opens up a new branch of structure-activity relationship studies.

The protonation macroconstants were also determined in excess of β-cyclodextrin and led to the conclusion that the amino group and its surroundings participate in the formation of the complex with β-cyclodextrin. The basicity of the phenolate group barely changed, so its role in complex formation is not decisive.

To prove the structure of the complex, we examined two-dimensional NMR spectra, allowing the establishment of a fitting model for these compounds, indicating the amino group and its surrounding region are embedded in the β-cyclodextrin cavity. Using a series of one-dimensional spectra recorded with increasing amounts of β-cyclodextrin, we also calculated the values of the stability constants and compared these values with circular dichroism measurements. Our in-depth characterization of the complex formed with β-cyclodextrin opens up the possibility for future, systematic formulation studies with a wide range of cyclodextrins.

Funding

We received no outside funding.

CRediT authorship contribution statement

Balázs Simon: Writing – review & editing, Writing – original draft, Methodology, Investigation, Conceptualization. **István Köteles:** Writing – review & editing, Methodology, Investigation. **Réka Kovács:** Writing – review & editing, Investigation, Formal analysis. **Márta Kraszni:** Writing – review & editing, Methodology, Formal analysis. **Péter Horváth:** Writing – review & editing, Methodology. **Sándor Hosztafi:** Writing – review & editing, Supervision, Resources, Methodology, Conceptualization. **Károly Mazák:** Writing – review & editing, Writing – original draft, Supervision, Project administration, Methodology, Formal analysis, Conceptualization.

Declaration of competing interest

The authors declare no conflict of interest.

Supplementary materials

Supplementary material associated with this article can be found, in the online version, at doi:10.1016/j.ejps.2025.107089.

Data availability

Data will be made available on request.

References

Aherne, G.W., Littleton, P., 1985. Morphine-6-glucuronide, an important factor in interpreting MORPHINE radioimmunoassays. The Lancet 27 (2 (8448)), 210–211.

Anton, B., Salazar, A., Flores, A., Matus, M., Marin, R., Hernandez, J.A., Leff, P., 2009. Vaccines against morphine/heroin and its use as effective medication for preventing relapse to opiate addictive behaviors. In: Human Vaccines, 5, pp. 214–229. https://doi.org/10.4161/hv.5.4.7556.

Bartole, E., Grätz, L., Littmann, T., Wifling, D., Seibel, U., Buschauer, A., Bernhardt, G., 2020. UR-DEBa242: a Py-5-labeled fluorescent multipurpose probe for investigations on the histamine H3 and H4 receptors. J. Med. Chem. 63 (10), 5297–5311. https://doi.org/10.1021/acs.jmedchem.0c00160.

Beike, J., Mertz, A., Blashke, G., Köhler, H., Brinkmann, B., 1998. A specific immunoassay for the determination of morphine, and its glucuronides in human blood. Int. J. Legal. Med. 112, 8–14.

Bremer, P.T., Janda, K.D., 2017. Conjugate vaccine immunotherapy for substance use disorder. Pharmacol. Rev. 69 (3), 298–315. https://doi.org/10.1124/pr.117.013904.

Bremer, P.T., Schlosburg, J.E., Banks, M.L., Steele, F.F., Zhou, B., Poklis, J.L., Janda, K. D., 2017. Development of a clinically viable Heroin vaccine. J. Am. Chem. Soc. 139 (25), 8601–8611. https://doi.org/10.1021/jacs.7b03334.

Bye, E., 1976. The crystal structure of morphine hydrate. Acta Chem. Scand. 30 (6 B), 549–554. https://doi.org/10.3891/ACTA.CHEM.SCAND.30B-0549.

Crone, T.A., Purdie, N., 1981. Circular dichroism spectra of opium alkaloids in aqueous Media. Anal. Chem. 53 (1), 17–21. https://doi.org/10.1021/AC00224A007/ASSET/AC00224A007.FP.PNG_V03.

de Robertis, A., Foti, C., Giuffrè, O., Sammartano, S., 2001. Dependence on ionic strength of polyamine protonation in NaCl aqueous solution. J. Chem. Eng. Data 46 (6), 1425–1435. https://doi.org/10.1021/JE010143G/ASSET/IMAGES/LARGE/JE010143GF00003.JPEG.

de Villiers, S.H.L., Lindblom, N., Kalayanov, G., Gordon, S., Baraznenok, I., Malmerfelt, A., Marcus, M.M., Johansson, A.M., Svensson, T.H., 2010. Nicotine hapten structure, antibody selectivity and effect relationships: results from a nicotine vaccine screening procedure. Vaccine 28 (10), 2161–2168. https://doi.org/10.1016/j.vaccine.2009.12.051.

Findlay, J.W.A., Butz, R.F., Jones, E.C., 1981. Relationships between immunogen structure and antisera specificity in the narcotic alkaloid series. In: CLINICAL CHEMISTRY, 27. https://academic.oup.com/clinchem/article/27/9/1524/5666505.

Gross, S.1, Grant, J.D., Wong, R., Schuster, R., Campbell, D.H., 1974. Critical Antigenic Determinants For Production Of Antibody To Distinguish Morphine From Heroin, Codeine And Dextromethorphan, 11. Pergamon Press Printed.

Gutman, E.S., Irvin, T.C., Morgan, J.B., Barrientos, R.C., Torres, O.B., Beck, Z., Matyas, G. R., Jacobson, A.E., Rice, K.C., 2021. Synthesis and immunological effects of C14-linked 4,5-epoxymorphinan analogues as novel heroin vaccine haptens. RSC. Chem. Biol. 2 (3), 835–842. https://doi.org/10.1039/d1cb00029b.

Haddou, T.Ben, Béni, S., Hosztafi, S., Malfacini, D., Calo, G., Schmidhammer, H., Spetea, M., 2014. Pharmacological investigations of N-substituent variation in morphine and oxymorphone: opioid receptor binding, signaling and antinociceptive activity. PLoS. One 9 (6). https://doi.org/10.1371/journal.pone.0099231.

Herndon, B.L., Paull, K., Baeder, D.H., Ringle, D.A., 1976. 325 Comparison of immljnogenicity of opiates bound to protein at different sites on the molecule: n-carboxy morphine-BSA. In: Pharmacological Research Communications, 8.

Hosztafi, S., Galambos, A.R., Köteles, I., Karádi, D., Fürst, S., Al-Khrasani, M., 2024. Opioid-based haptens: development of immunotherapy. In: International Journal of Molecular Sciences, 25. Multidisciplinary Digital Publishing Institute (MDPI). https://doi.org/10.3390/ijms25147781.

Huang, C.Y., 1982. Determination of binding stoichiometry by the continuous variation method: the job plot. Meth. Enzymol. 87 (C), 509–525. https://doi.org/10.1016/S0076-6879(82)87029-8.

Huang, C.Y., Zhou, R., Yang, D.C.H., Chock, P.B., 2002. Application of the continuous variation method to cooperative interactions: mechanism of Fe(II) - ferrozine chelation and conditions leading to anomalous binding ratios. Biophys. Chem. 100 (1–3), 143–149. https://doi.org/10.1016/S0301-4622(02)00275-2.

Humphreys, K., Shover, C.L., Andrews, C.M., Bohnert, A.S.B., Brandeau, M.L., Caulkins, J.P., Chen, J.H., Cuéllar, M.F., Hurd, Y.L., Juurlink, D.N., Koh, H.K., Krebs, E.E., Lembke, A., Mackey, S.C., Larrimore Ouellette, L., Suffoletto, B., Timko, C., 2022. Responding to the opioid crisis in North America and beyond: recommendations of the Stanford–Lancet Commission. In: The Lancet, 399. Elsevier B.V., pp. 555–604. https://doi.org/10.1016/S0140-6736(21)02252-2

Ingham, K.C., 1975. On the application of Job's method of continuous variation to the stoichiometry of protein-ligand complexes. Anal. Biochem. 68 (2), 660–663. https://doi.org/10.1016/0003-2697(75)90666-1.

Jalah, R., Torres, O.B., Mayorov, A.V., Li, F., Antoline, J.F.G., Jacobson, A.E., Rice, K.C., Deschamps, J.R., Beck, Z., Alving, C.R., Matyas, G.R., 2015. Efficacy, but not antibody titer or affinity, of a Heroin hapten conjugate vaccine correlates with increasing hapten densities on tetanus toxoid, but not on CRM197 carriers. Bioconjug. Chem. 26 (6), 1041–1053. https://doi.org/10.1021/acs.bioconjchem.5b00085.

Judd, D., King, C.R., Galke, C., 2023. The Opioid Epidemic: a review of the contributing factors, negative consequences, and best practices. Cureus. https://doi.org/10.7759/cureus.41621.

Bonese, K.F., Wainer, B.H., Fitch, F.W., Rothberg, R.M., Schuster, C.R., 1974. Changes in heroin self- administration by a rhesus monkey after morphine immunisation. Nature 253.

Kimishima, A., Wenthur, C.J., Zhou, B., Janda, K.D., 2017. An advance in prescription opioid vaccines: overdose mortality reduction and extraordinary alteration of drug half-life. ACS. Chem. Biol. 12 (1), 36–40. https://doi.org/10.1021/acschembio.6b00977.

Kiss, E., Szabó, V.A., Horváth, P., 2019. Simple circular dichroism method for selection of the optimal cyclodextrin for drug complexation. J. Incl. Phenom. Macrocycl. Chem. 95 (3–4), 223–233. https://doi.org/10.1007/S10847-019-00938-2.

Kręzel, A., Bal, W., 2004. A formula for correlating pKa values determined in D2O and H2O. J. Inorg. Biochem. 98 (1). https://doi.org/10.1016/j.jinorgbio.2003.10.001.

Lee, J., Kresina, T.F., Campopiano, M., Lubran, R., Clark, H.W., 2015. Use of pharmacotherapies in the treatment of alcohol use disorders and opioid dependence in primary care. In: BioMed Research International, 2015. Hindawi Publishing Corporation. https://doi.org/10.1155/2015/137020.

Loftsson, T., Duchêne, D., 2007. Cyclodextrins and their pharmaceutical applications. Int. J. Pharm. 329 (1–2), 1–11. https://doi.org/10.1016/J.IJPHARM.2006.10.044.

Malik, A., Hosztafi, S., Vincze, A., Marton, A., Kraszni, M., Balogh, G.T., Noszál, B., Mazák, K., 2024. Characterization of opioid agonist morphine derivatives with emphasis on medicinal chemistry. ChemMedChem. https://doi.org/10.1002/CMDC.202400654.

Matyas, G.R., Rice, K.C., Cheng, K., Li, F., Antoline, J.F.G., Iyer, M.R., Jacobson, A.E., Mayorov, A.V., Beck, Z., Torres, O.B., Alving, C.R., 2014. Facial recognition of heroin vaccine opiates: type 1 cross-reactivities of antibodies induced by hydrolytically stable haptenic surrogates of heroin, 6-acetylmorphine, and morphine. Vaccine 32 (13), 1473–1479. https://doi.org/10.1016/j.vaccine.2014.01.028.

May, E.L., Jacobson, A.E., Mattson, M.V, Traynor, J.R., Woods, J.H., Harris, L.S., Bowman, E.R., Aceto, M.D., 2000. Synthesis and in Vitro and in Vivo Activity of-N-Alkynyl-, And-N-Cyanoalkyl-5,9-Dimethyl-2′-Hydroxy-6,7-Benzomorphan Homologues. https://doi.org/10.1021/jm000317.

Mazák, K., Hosztafi, S., Rácz, Á., Noszál, B., 2009. Structural and physicochemical profiling of morphine and related compounds of therapeutic interest. Mini-Rev. Med. Chem. 9, 984–995.

Mazák, K., Noszál, B., 2016. Advances in microspeciation of drugs and biomolecules: species-specific concentrations, acid-base properties and related parameters. J. Pharm. Biomed. Anal. 130, 390–403. https://doi.org/10.1016/j.jpba.2016.03.053.

Mazák, K., Noszál, B., Hosztafi, S., 2019. Advances in the physicochemical profiling of opioid compounds of therapeutic interest. ChemistryOpen. 8 (7), 879–887. https://doi.org/10.1002/open.201900115.

Mumba, M.N., Findlay, L.J., Snow, D.E., 2018. Treatment options for opioid use disorders: a review of the relevant literature. In: Journal of Addictions Nursing, 29. Lippincott Williams and Wilkins, pp. 221–225. https://doi.org/10.1097/JAN.0000000000000241.

Olofson, R.A., Martz, J.T., Senet, J.P., Piteau, M., Malfroot, T., 1984. A new reagent for the selective, high-yield N-dealkylation of tertiary amines: improved syntheses of naltrexone and nalbuphine. J. Org. Chem. 49 (11), 2081–2082. https://doi.org/10.1021/jo00185a072.

Ötvös, F., Szűcs, E., Urai, Á., Köteles, I., Szabó, P.T., Varga, Z.K., Gombos, D., Hosztafi, S., Benyhe, S., 2023. Synthesis and biochemical evaluation of 17-N-beta-aminoalkyl-4,5α-epoxynormorphinans. Sci. Rep. 13 (1). https://doi.org/10.1038/s41598-023-46317-3.

Pálla, T., Kolompár, Z., Mazák, K., Mirzahosseini, A., Noszál, B., 2023. Estimating the bias of model compounds for the determination of species-specific protonation constants. ACS. Omega 9 (1), 896–902. https://doi.org/10.1021/acsomega.3c06994.

Pravetoni, M., Le Naour, M., Harmon, T.M., Tucker, A.M., Portoghese, P.S., Pentel, P.R., 2012. An oxycodone conjugate vaccine elicits drug-specific antibodies that reduce oxycodone distribution to brain and hot-plate analgesia. J. Pharmacol. Exp. Therap. 341 (1), 225–232. https://doi.org/10.1124/jpet.111.189506.

Ramakrishnan, M., Kinsey, B.M., Singh, R.A., Kosten, T.R., Orson, F.M., 2014. Hapten optimization for cocaine vaccine with improved cocaine recognition. Chem. Biol. Drug Des. 84 (3), 354–363. https://doi.org/10.1111/cbdd.12326.

Brown, Richard T., Carter, Neil E., Lumbard, Keith W., Scheimann, Feodor, 1995. Synthesis of a Morphine-6-Glucuronide Hapten, N-(4-Aminobutyl)normorphine-6-glucuronide, and Related Haptens.

Saokham, P., Muankaew, C., Jansook, P., Loftsson, T., 2018. Solubility of cyclodextrins and drug/cyclodextrin complexes. Molecules. 23 (5). https://doi.org/10.3390/MOLECULES23051161.

Subasinghe, K.R., Jackson, W.R., Young, J.F., Papanastasiou, M., Jarrott, B., 2004. Non-CNS acting opiates bearing guanidino substituents. Aust. J. Chem. 57 (5), 427–438. https://doi.org/10.1071/CH03199.

Stowe, G.N., Vendruscolo, L.F., Edwards, S., Schlosburg, J.E., Misra, K.K., Schulteis, G., Mayorov, A.V., Zakhari, J.S., Koob, G.F., Janda, K.D., 2011. A vaccine strategy that induces protective immunity against heroin. J. Med. Chem. 54 (14), 5195–5204. https://doi.org/10.1021/jm200461m.

Stowe, G.N., E. Schlosburg, J., F. Vendruscolo, L., Edwards, S., K. Misra, K., Schulteis, G., S. Zakhari, J., F. Koob, G., D. Janda, K., 2012. Developing a vaccine against multiple psychoactive targets: a case study of Heroin. CNS & Neurol. Disorders - Drug Targets 10 (8), 865–875. https://doi.org/10.2174/187152711799219316.

Sulima, A., Jalah, R., Antoline, J.F.G., Torres, O.B., Imler, G.H., Deschamps, J.R., Beck, Z., Alving, C.R., Jacobson, A.E., Rice, K.C., Matyas, G.R., 2018. A stable heroin analogue that can serve as a vaccine hapten to induce antibodies that block the effects of Heroin and its metabolites in rodents and that cross-react immunologically with related drugs of abuse. J. Med. Chem. 61 (1), 329–343. https://doi.org/10.1021/acs.jmedchem.7b01427.

Tűz, B., Noszál, B., Hosztafi, S., Mazák, K., 2022. B-cyclodextrin complex formation and protonation equilibria of morphine and other opioid compounds of therapeutic interest. Eur. J. Pharmaceut. Sci. 171 (January), 0–10. https://doi.org/10.1016/j.ejps.2022.106120.

Usagawa, T., Itoh, Y., Hifumi, E., Takeyasu, A., Nakahara, Y., Uda, T., 1993. Characterization of morphine-specific monoclonal antibodies showing minimal cross-reactivity with codeine. J. lmmunol. Methods 157.

Volkow, N.D., McLellan, A.T., 2016. Opioid abuse in chronic pain — Misconceptions and mitigation strategies. New England J. Med. 374 (13), 1253–1263. https://doi.org/10.1056/nejmra1507771.

Wang, M., Irvin, T.C., Herdman, C.A., Hanna, R.D., Hassan, S.A., Lee, Y.S., Kaska, S., Crowley, R.S., Prisinzano, T.E., Withey, S.L., Paronis, C.A., Bergman, J., Inan, S., Geller, E.B., Adler, M.W., Kopajtic, T.A., Katz, J.L., Chadderdon, A.M., Traynor, J.R., Rice, K.C., 2020. The intriguing effects of substituents in the N-phenethyl moiety of norhydromorphone: a bifunctional opioid from a set of “tail wags dog” experiments. Molecules. 25 (11). https://doi.org/10.3390/molecules25112640.

WHO EML 23rd List, 2023, 2023. http://apps.who.int/bookorders.

Wolframalpha. Available online: https://www.wolframalpha.com/examples/mathematics/algebra (accessed on 19 March 2024). (n.d.).

Xiao, M., Yang, Q., Liang, Z., Puxty, G., He, X., Conway, W., 2018. Protonation constants of diamines using NMR spectroscopy for CO2 capture processes. In: GHGT 2018 - 14th International Conference on Greenhouse Gas Control Technologies. https://doi.org/10.2139/SSRN.3366312.